DVCS and Electron Ion Collider

Igor Korover

Massachusetts Institute of Technology

Center for Frontiers in Nuclear Science

The Quest to Understand the Fundamental Structure of Matter

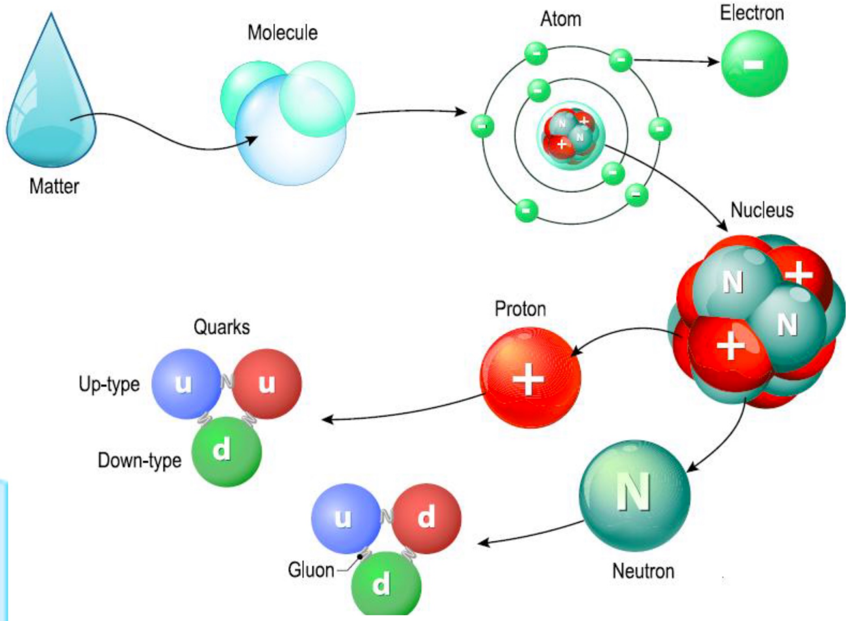

Diffractive imaging

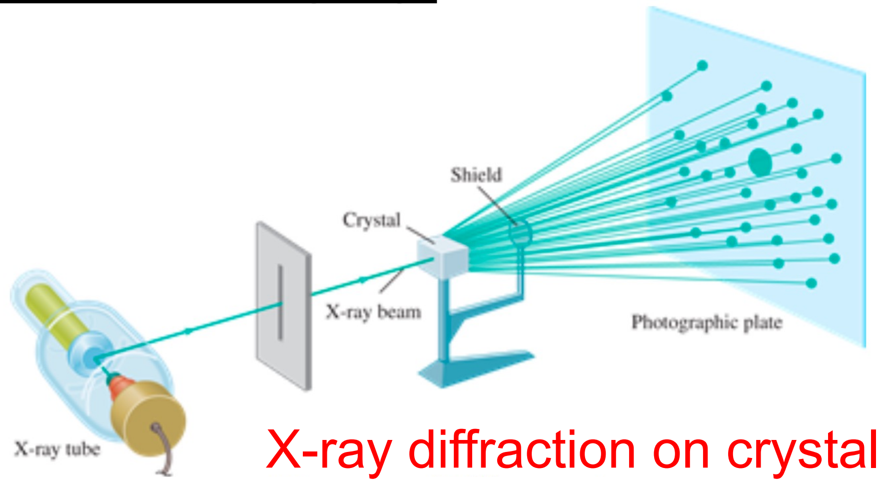

X-ray diffraction on crystals

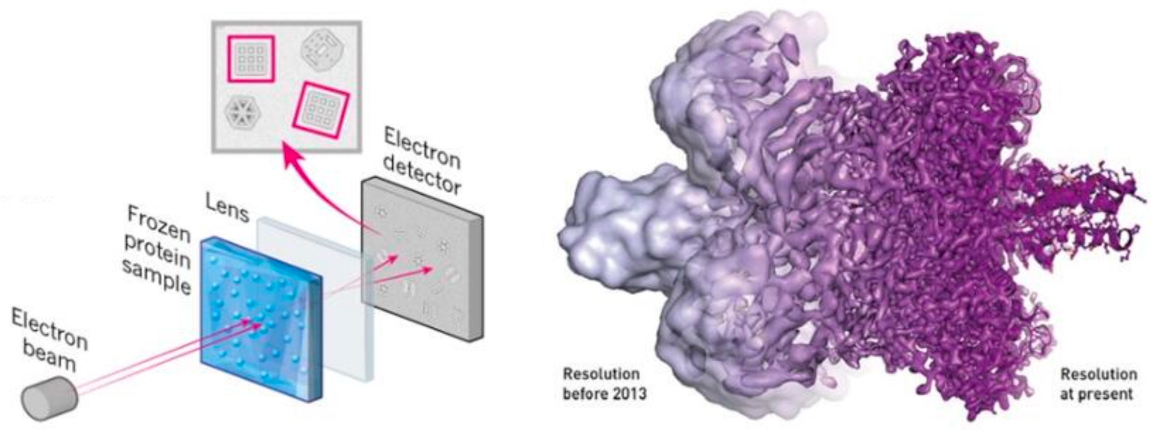

Electron diffraction on protein

The Electron <u>Microscopes</u>

SLAC, HERA, JLab, EIC

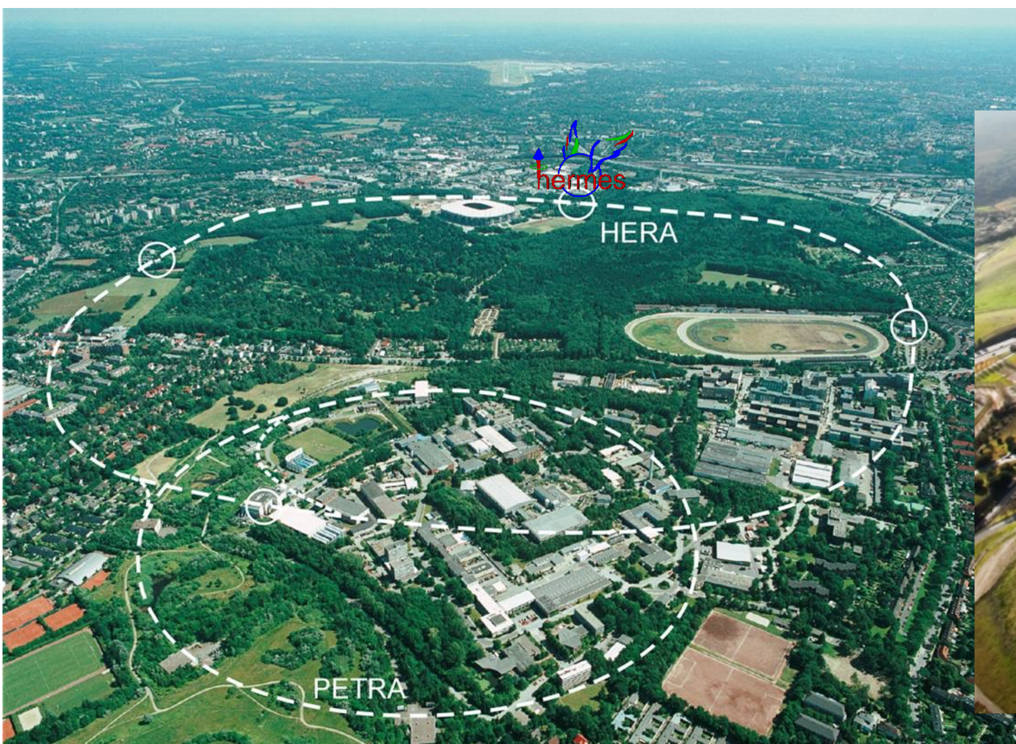

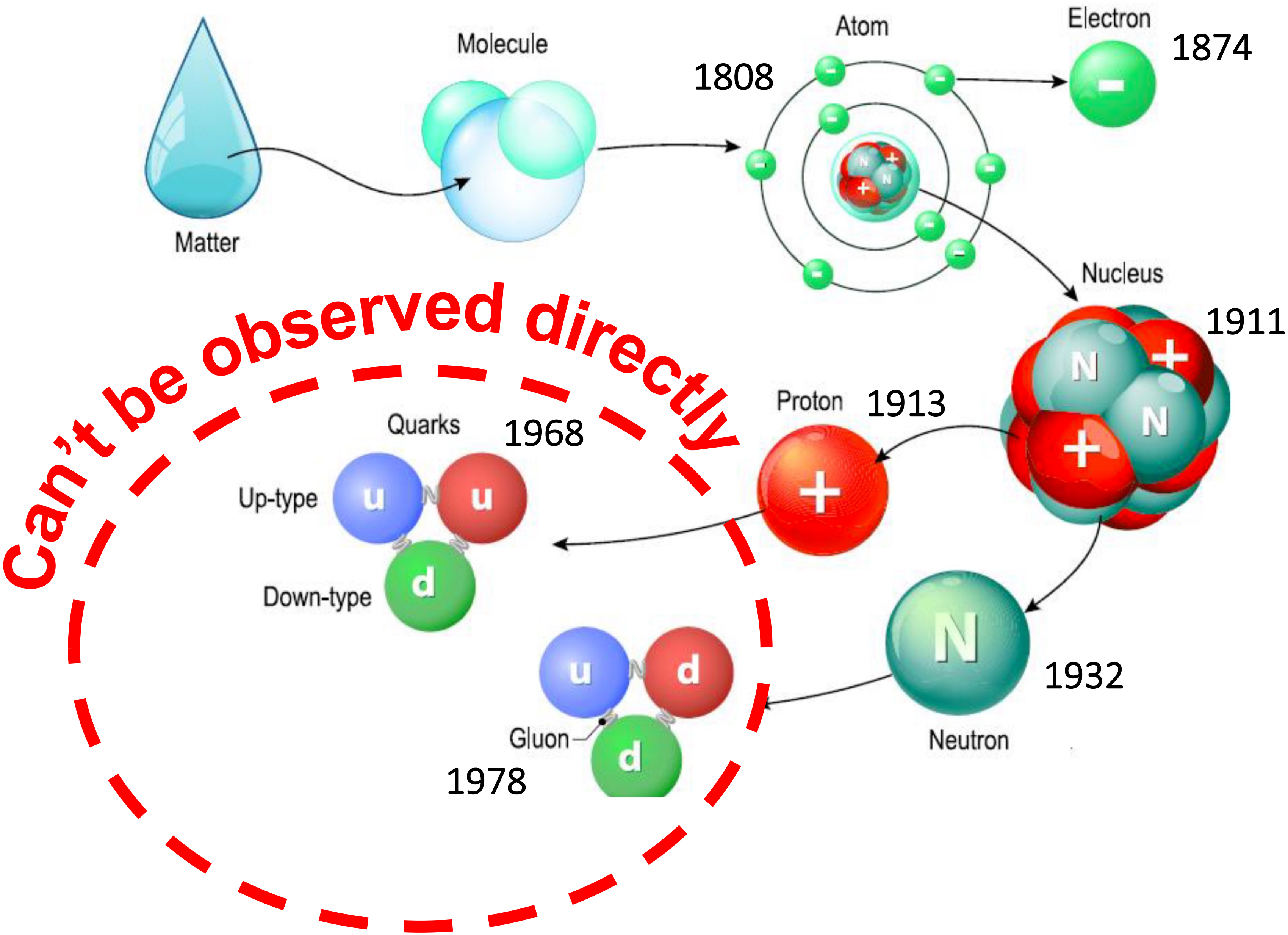
Matter
Molecule
Atom
1808
Electron
1874
Nucleus
1911
Proton
1913
Neutron
1932
Quarks
1968
Up-type
Down-type
Gluon
1978
Can't be observed directly

Proton Viewed in High Energy Electron Scattering: 1 Longitudinal Dimension

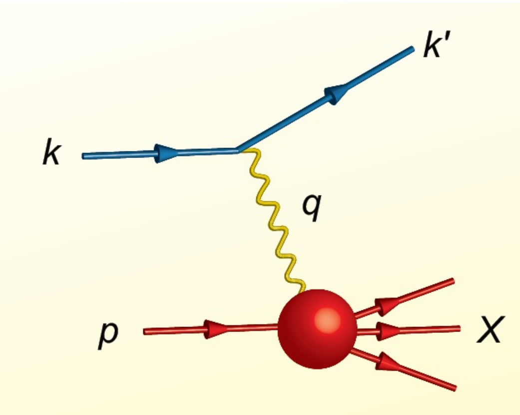

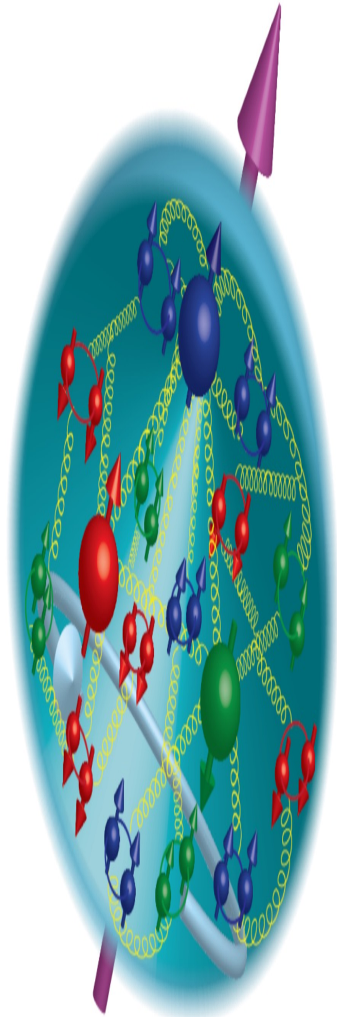

$$x_B = \frac{Q^2}{2 \cdot m_p \cdot \upsilon}$$

- Viewed from boosted frame, length contracted by

$$\gamma_{Breit} = \sqrt{1 + \frac{Q^2}{4M^2}}$$

- Internal motion of the nucleon's constituents is slowed down by time dilation – the instantaneous charge distribution of the nucleon is seen.
- In boosted frame x_B is understood as the longitudinal momentum fraction

  valence quarks: $0.1 < x_B < 1$

  sea quarks: $x_B < 0.1$

J. Bjorken, SLAC-PUB-0571 March 1969

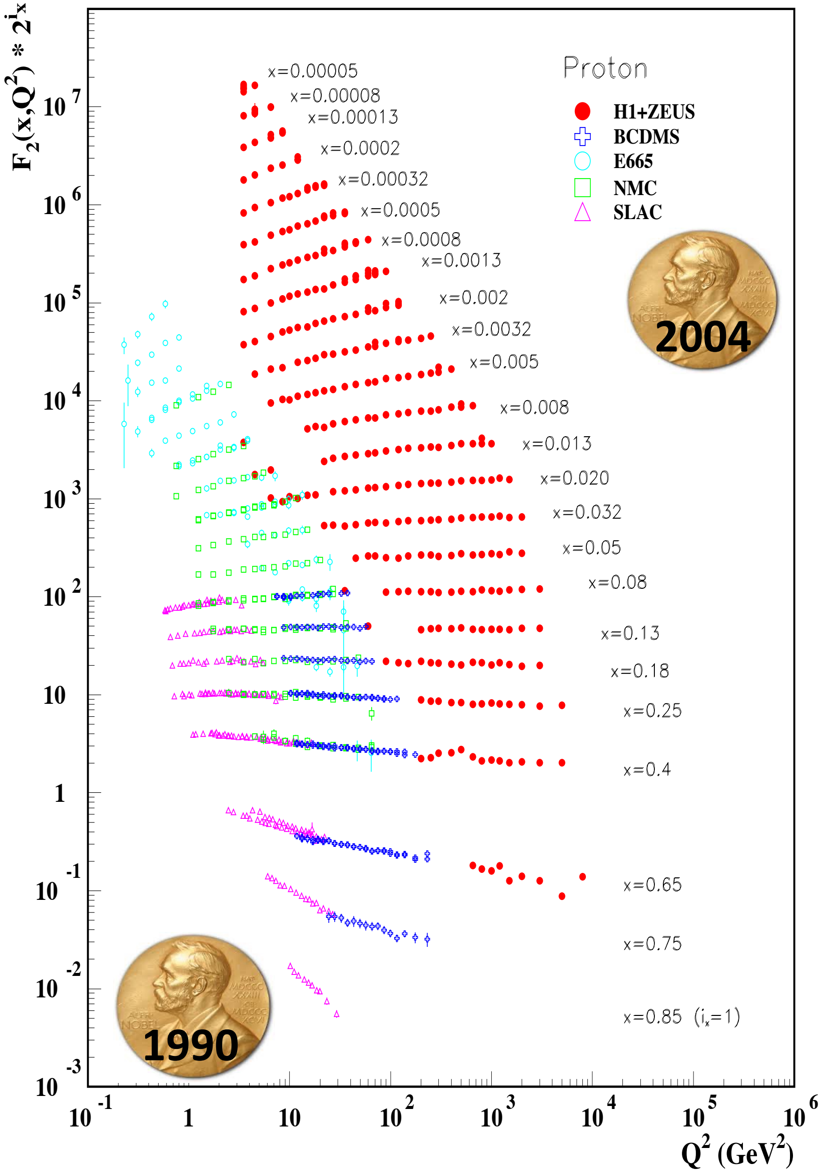

Quark Structure of Nucleon from High-Energy Lepton Scattering

e-p cross section ≈ $\sigma_{Mott} \bullet F_2(x, Q^2)$

- Snap shots of the charged structure of the proton taken in the boosted frame
- *1/Q* spatial resolution
- QCD prescribes evolution with Q^2 which connects quarks and gluons

Proton Tomography: 2 New Dimensions Transverse to Longitudinal Momentum

Structure mapped in terms of
b$_T$ = transverse position
k$_T$ = transverse momentum

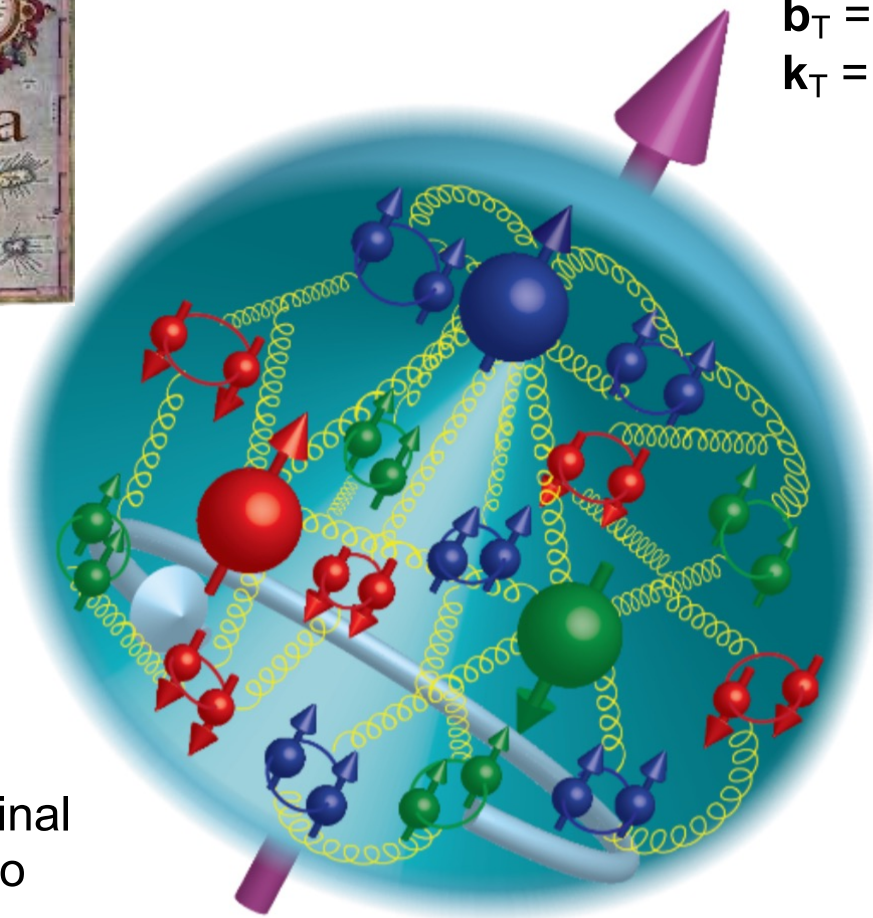

Goal:
Unprecedented
21st Century Imaging
of Hadronic Matter

Direction of longitudinal momentum normal to plane of slide

Valence Quarks: JLab 12 GeV
Sea Quarks and Gluons: EIC

3D Partonic Picture

Theorists have developed a powerful formalism for studying the 3D partonic picture of the nucleon and the nucleus. It is encoded in **Generalized Parton Distributions** and **Transverse Momentum Dependent Distributions**

Wigner distribution

$$W(\mathbf{p}, \mathbf{x})$$

Transverse Momentum Dependent distributions

$d^3 r$

$d^3 p$

Generalized Parton Distributions

Orbital motion accessible!

$$f(x, \mathbf{k}_\perp)$$

$$H(x, \xi, t)$$

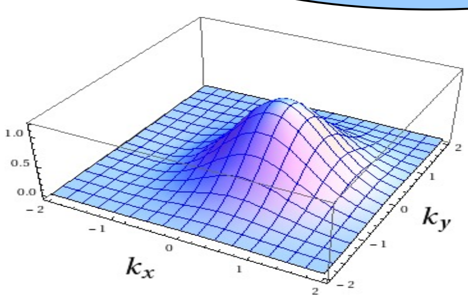

SIDIS

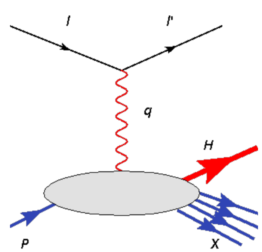

DES

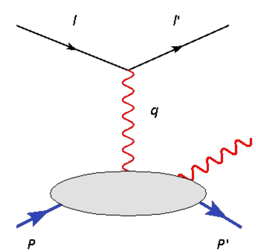

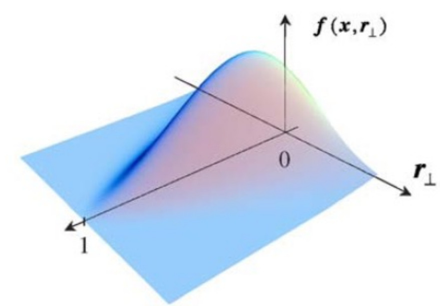

Generalized Parton Distributions

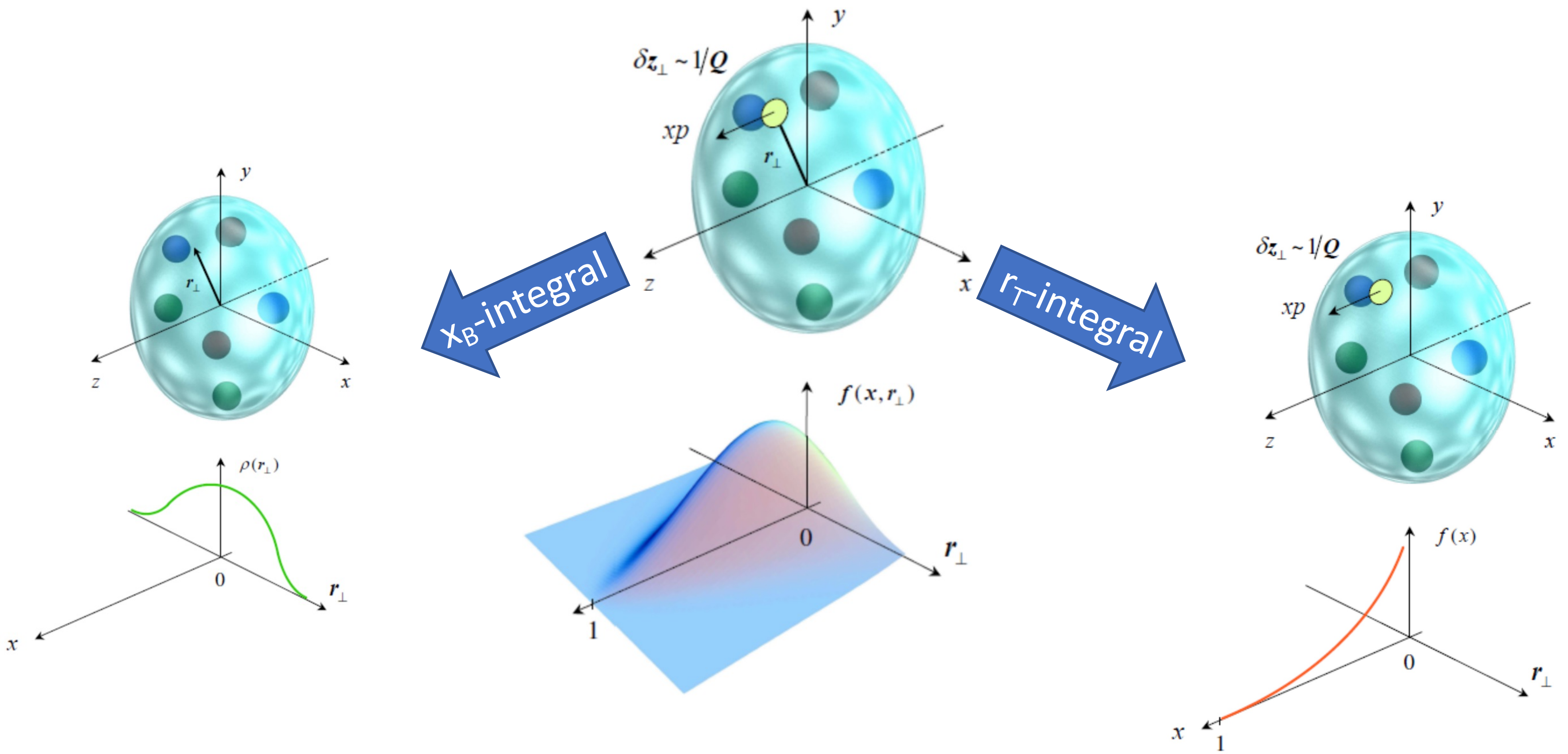

<u>EM structure</u>
Form factors, **<u>transverse</u>**
charge & current distributions

Nobel prize 1961-
Hofstadter

<u>Quark-gluon structure</u>
<u>longitudinal</u> momentum
& helicity distributions

Nobel prize 1990 -
Friedman, Kendall, Taylor

A world in a Function:
Generalized Parton Distributions (GPDs)

- Nucleon Spin

$$J_q = \frac{1}{2}\Delta\Sigma + L_q = \frac{1}{2}[A_{q,g}(0) + B_{q,g}(0)]$$

$$\int_{-1}^{1} dx x[H(x,\xi,\Delta^2) + E(x,\xi,\Delta^2)] = A(\Delta^2) + B(\Delta^2)$$

R. G. Milner and R. Ent, Visualizing the Proton (2022)

- 3D Tomography

$$q(x, \mathbf{b}_\perp) = \int \frac{d^2\mathbf{\Delta}_\perp}{(2\pi)^2} H_q(x, -\mathbf{\Delta}_\perp{}^2) e^{-i\mathbf{b}_\perp \cdot \mathbf{\Delta}_\perp}$$

- Origin of Visible Mass

- Nucleon Energy-Momentum Tensor (EMT)

$$M_2^q(t) + \frac{4}{5} d_1(t)\xi^2 = \frac{1}{2}\int_{-1}^{1} dx x H^q(x,\xi,t)$$

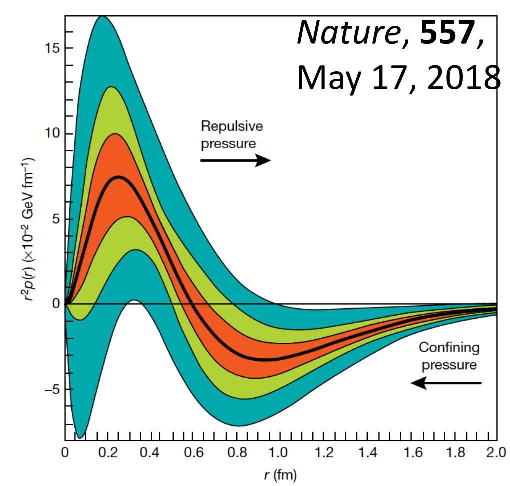

X. Ji, Phys. Rev. Lett. 74, 1071 (1995)

X. Ji, Phys. Rev. Lett. 78, 610 (1997)

M.Burkardt (2002)

Deeply **V**irtual **C**ompton **S**cattering (**DVCS**)

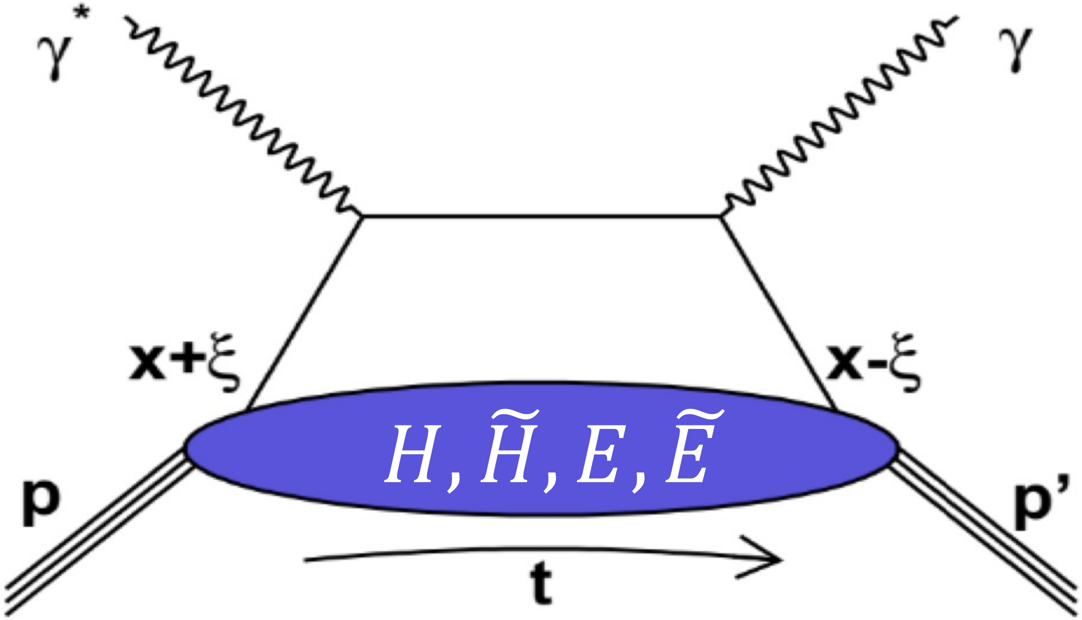

Deeply Virtual Compton Scattering (DVCS)

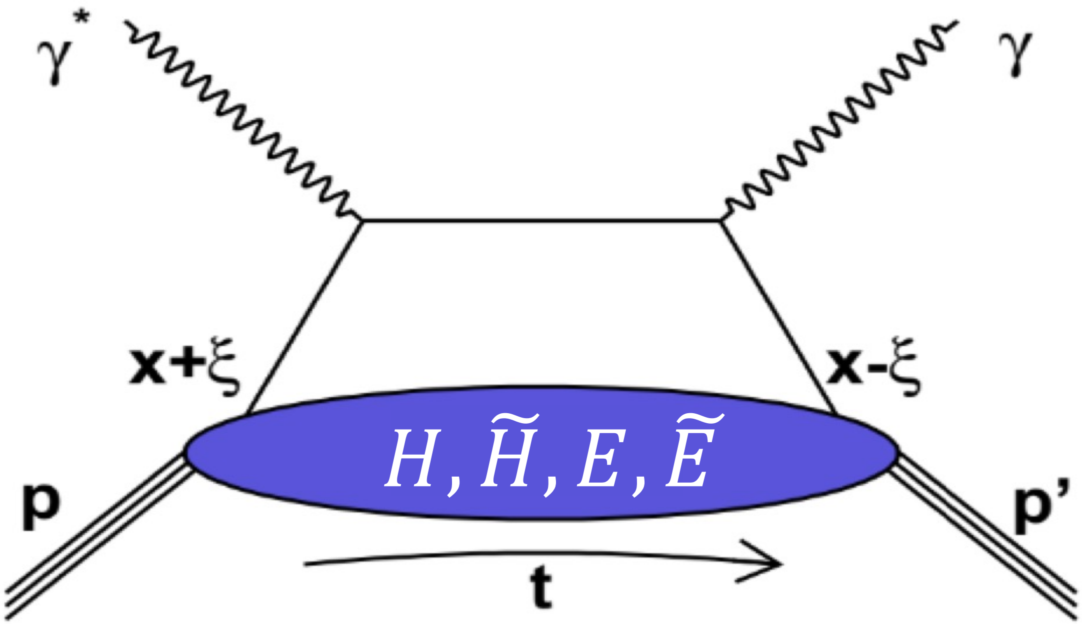

x – longitudinal quark momentum fraction

2ξ – longitudinal momentum transfer

t – Fourier conjugate to transverse impact parameter

Amplitude is given by four GPDs:

GPDs depend on 3 kinematic variables, e.g. *(x, ξ, t)*, that describe the internal nucleon dynamics.

$$i\mathcal{M} = -i\sum_q (|e|Q_q)^2 \epsilon^*_\mu \epsilon_\nu \Bigg\{$$

$$(p_1^\mu p_2^\nu + p_1^\nu p_2^\mu - g_\perp^{\mu\nu}) \int_{-1}^{1} dx \left[\frac{1}{x-\xi+i\epsilon} + \frac{1}{x+\xi-i\epsilon}\right] \times \frac{1}{2P^+}\left[H^q(x,\xi,t)\bar{u}(p')\gamma^+ u(p) + E^q(x,\xi,t)\bar{u}(p') i\sigma^{+\alpha}\frac{\Delta_\alpha}{2m_N}u(p)\right]$$

$$+i\epsilon^{\mu\nu+-}\int_{-1}^{1} dx \left[\frac{1}{x+\xi-i\epsilon} - \frac{1}{x-\xi+i\epsilon}\right] \times \frac{1}{2P^+}\left[\tilde{H}^q(x,\xi,t)\bar{u}(p')\gamma^+\gamma_5 u(p) + \tilde{E}^q(x,\xi,t)\bar{u}(p')\gamma_5\frac{\Delta^+}{2m_N}u(p)\right]\Bigg\}$$

Deeply Virtual Compton Scattering

$$e + p \rightarrow e' + p' + \gamma$$

Simple reaction… but:

- Low cross-section
- Large non-DVCS background
- Exclusivity requirement
- 4-dimentional extraction required

➔ Ideally suited for a high-luminosity, high-resolution, large acceptance experimental setups.

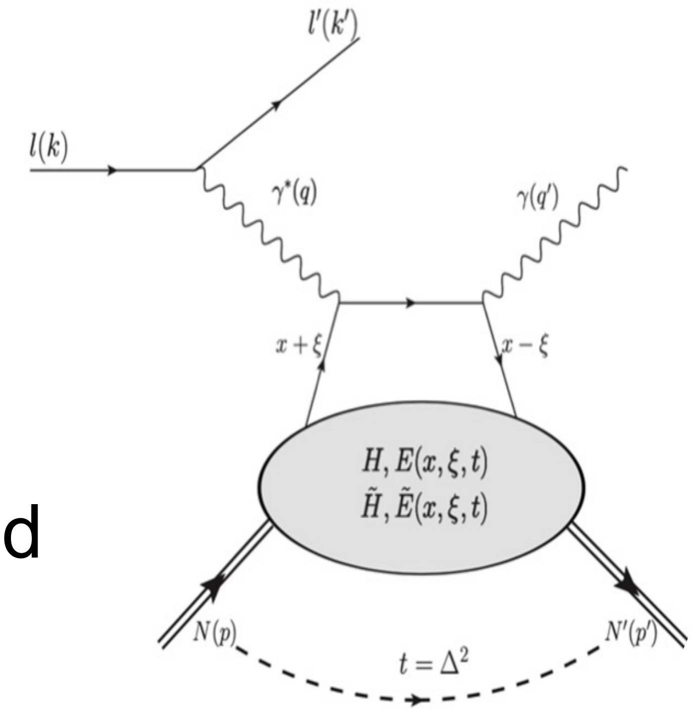

DVCS

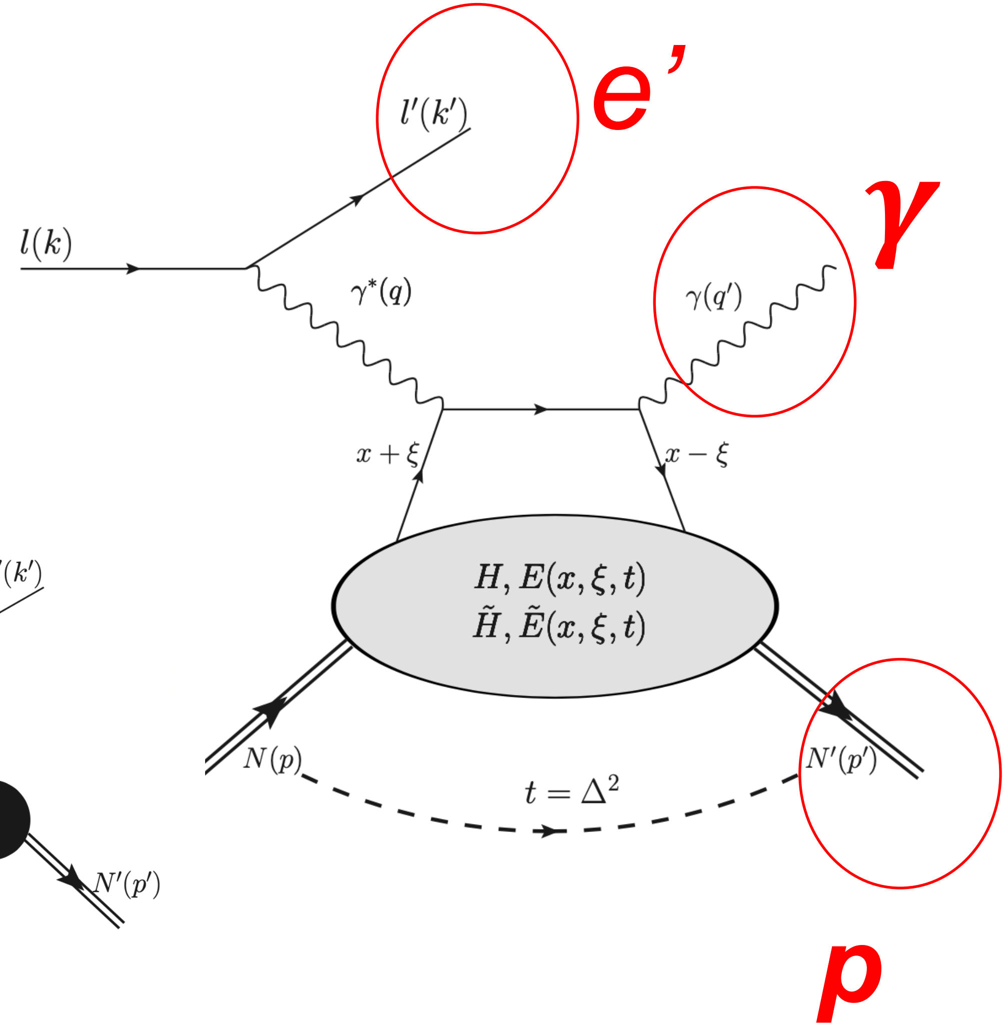

Irreducible Background

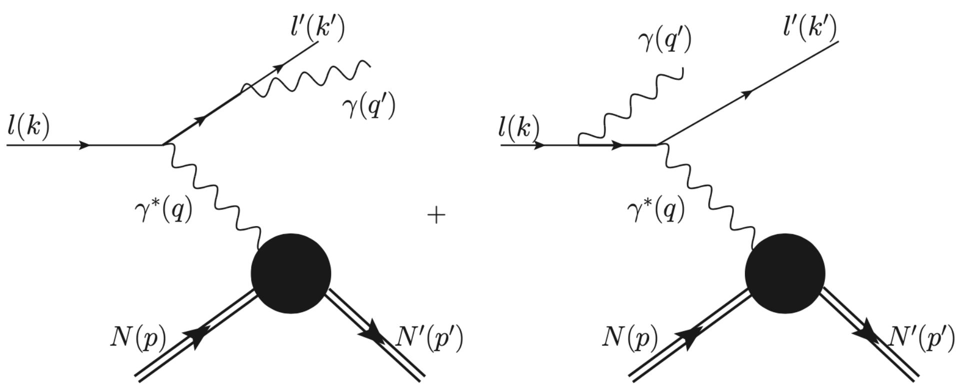

$$\frac{d\sigma^{\mathrm{TOT}}(x_{\mathrm{B}}, t, \mathcal{Q}^2|y)}{dt} \equiv \frac{1}{\Gamma(x_{\mathrm{B}}, \mathcal{Q}^2|y)} \int_{-\pi}^{\pi} d\phi \, \frac{d\sigma^{ep\to ep\gamma}(x_{\mathrm{B}}, t, \mathcal{Q}^2|y)}{dt d\phi dx_{\mathrm{B}} d\mathcal{Q}^2} \times dx_{\mathrm{B}} d\mathcal{Q}^2$$

$$= \frac{d\sigma^{\mathrm{BH}}(x_{\mathrm{B}}, t, \mathcal{Q}^2|y)}{dt} \pm \frac{d\sigma^{\mathrm{INT}}(x_{\mathrm{B}}, t, \mathcal{Q}^2|y)}{dt} + \frac{d\sigma^{\mathrm{DVCS}}(x_{\mathrm{B}}, t, \mathcal{Q}^2|y)}{dt}$$

Jefferson Lab

Absolute cross section/ BSA measurement

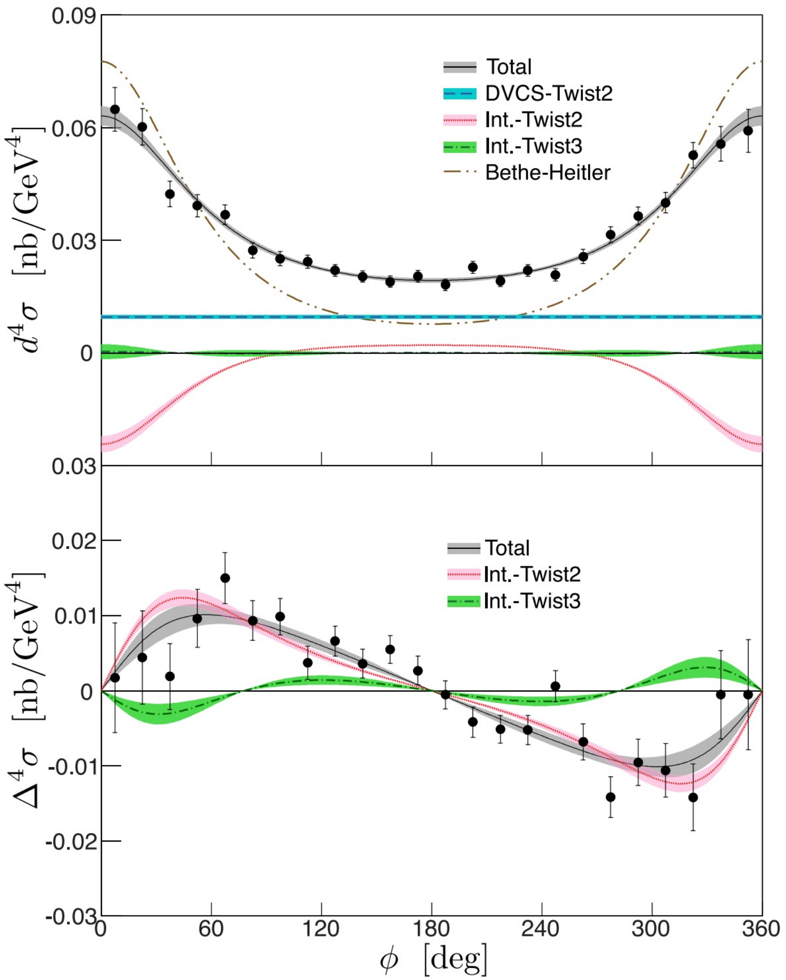

PHYSICAL REVIEW C 92, 055202 (2015)

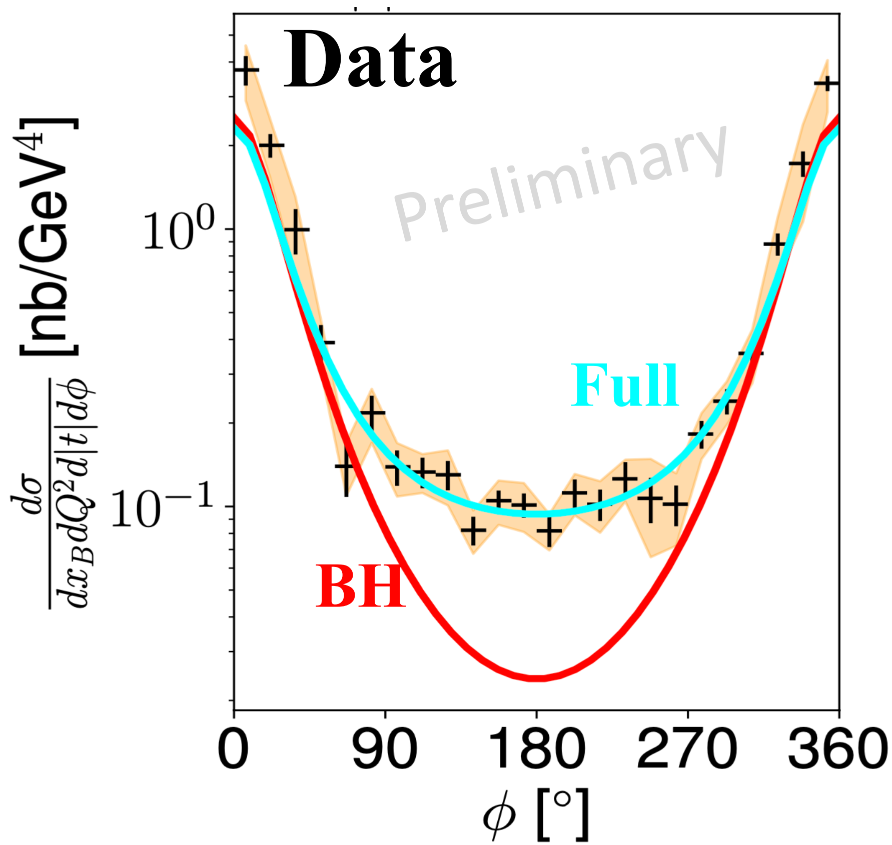

PhD Thesis, MIT

Jefferson Lab

Absolute

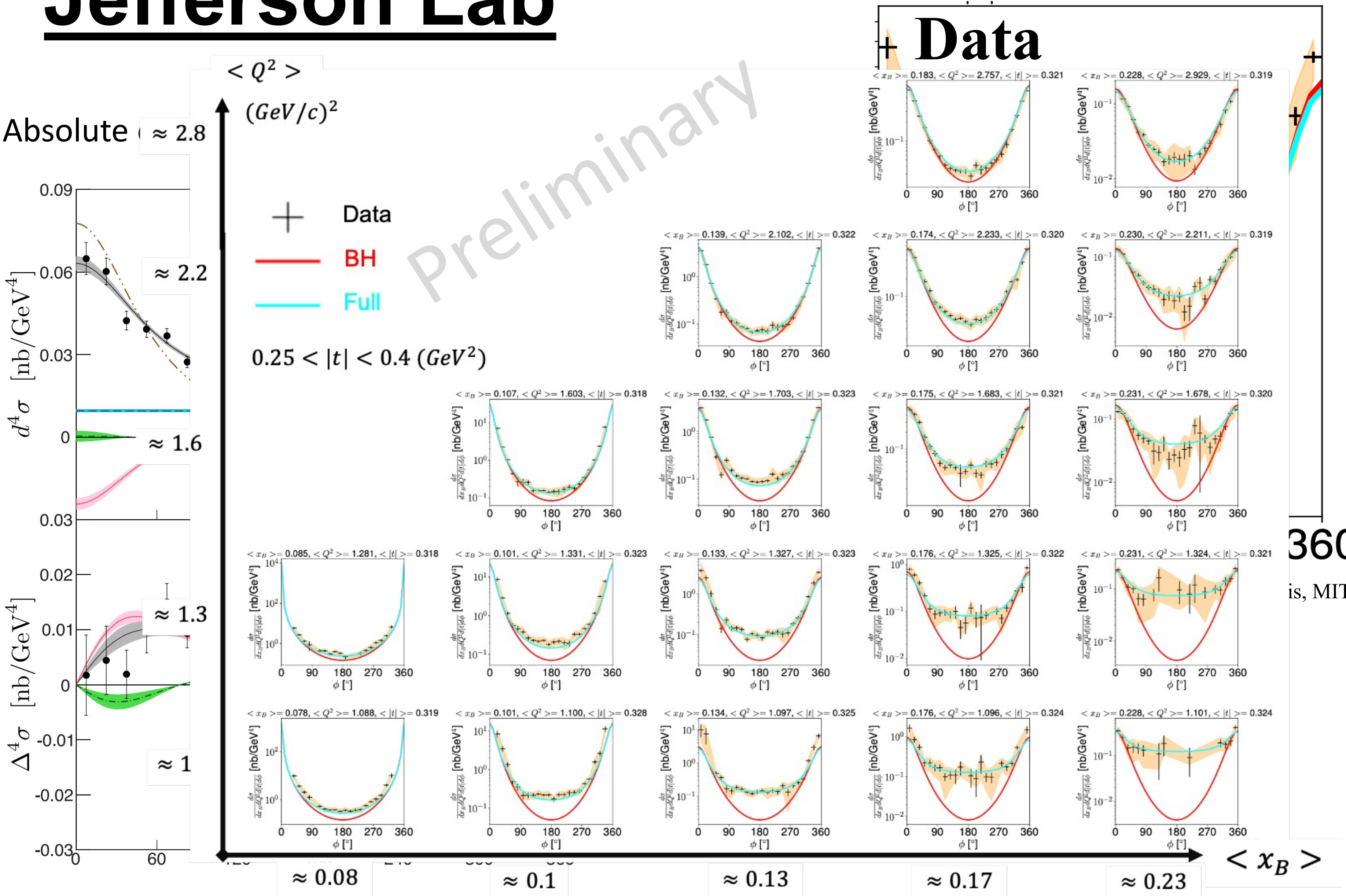

PHYSICAL REVIEW C 92, 055202 (2015)

DVCS phase space

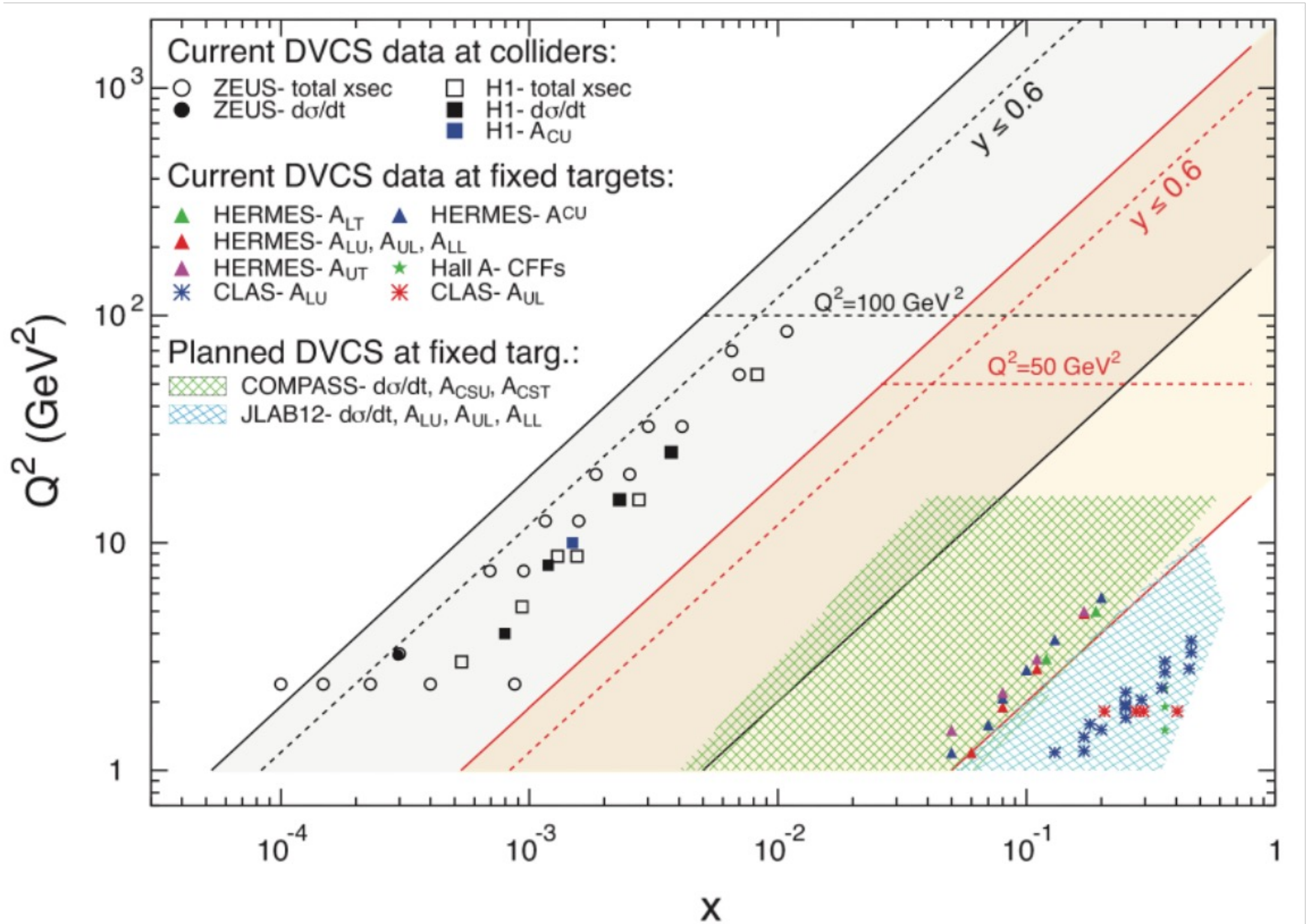

J. High Energ. Phys. **2013**, 93 (2013)

Polarized ep (eA) collider located at Brookhaven National Lab

DOE project, set to revolutionize our understanding of QCD

p: 40 – 275 GeV
e: 5 – 18 GeV

Data taking starting 2031/32

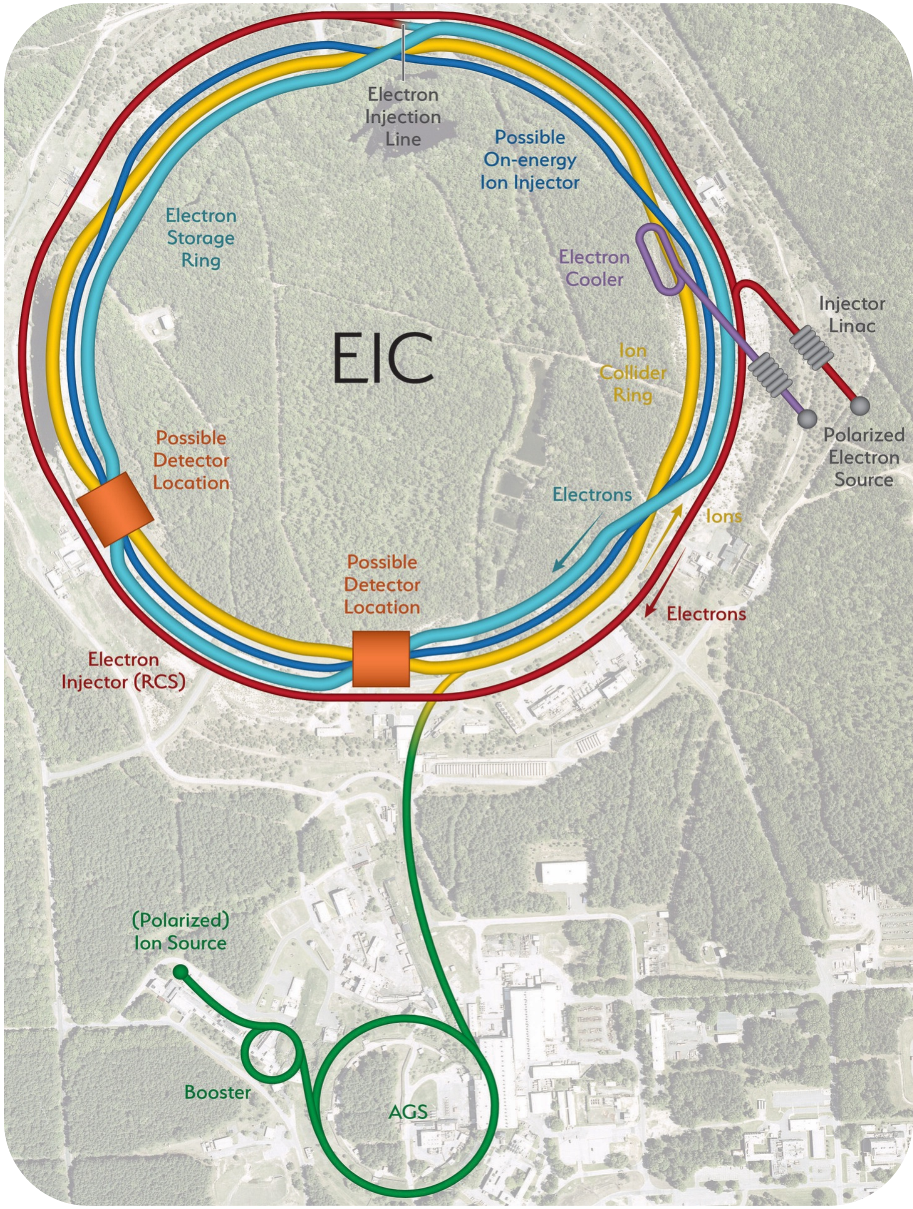

Origin of Spin

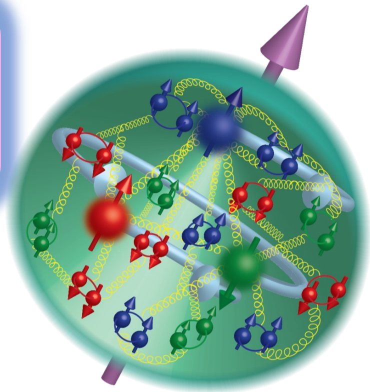

Femtography

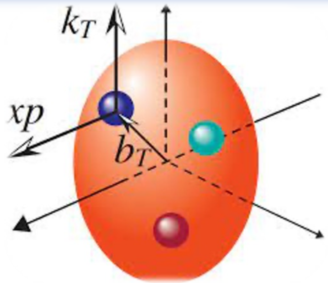

EIC Core Science

Standard Model

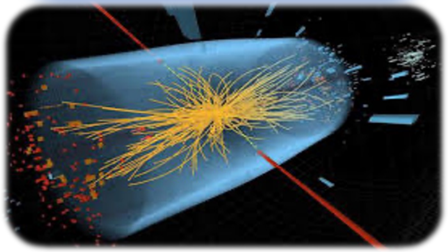

Origin of Mass

Dense Gluons

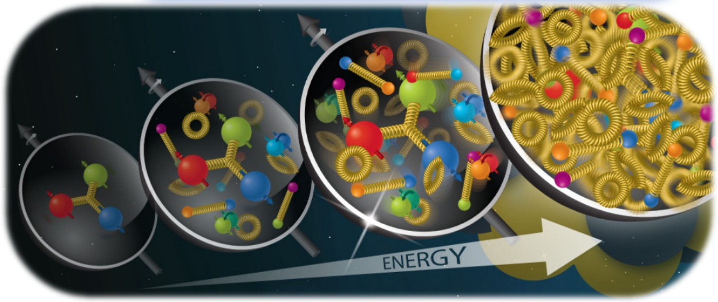

Pseudo data: no detector simulation

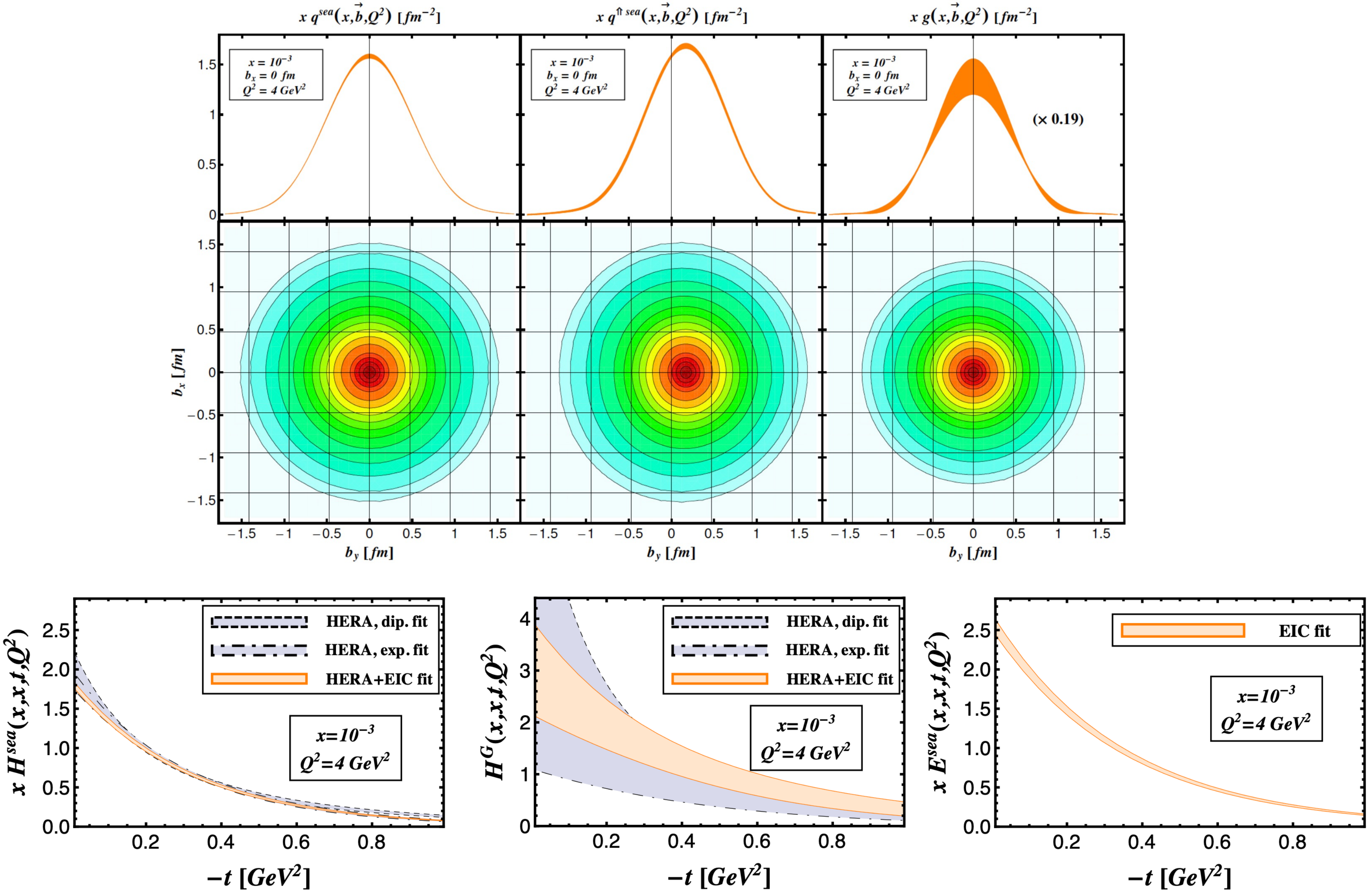

J. High Energ. Phys. **2013**, 93 (2013)

EIC central detector

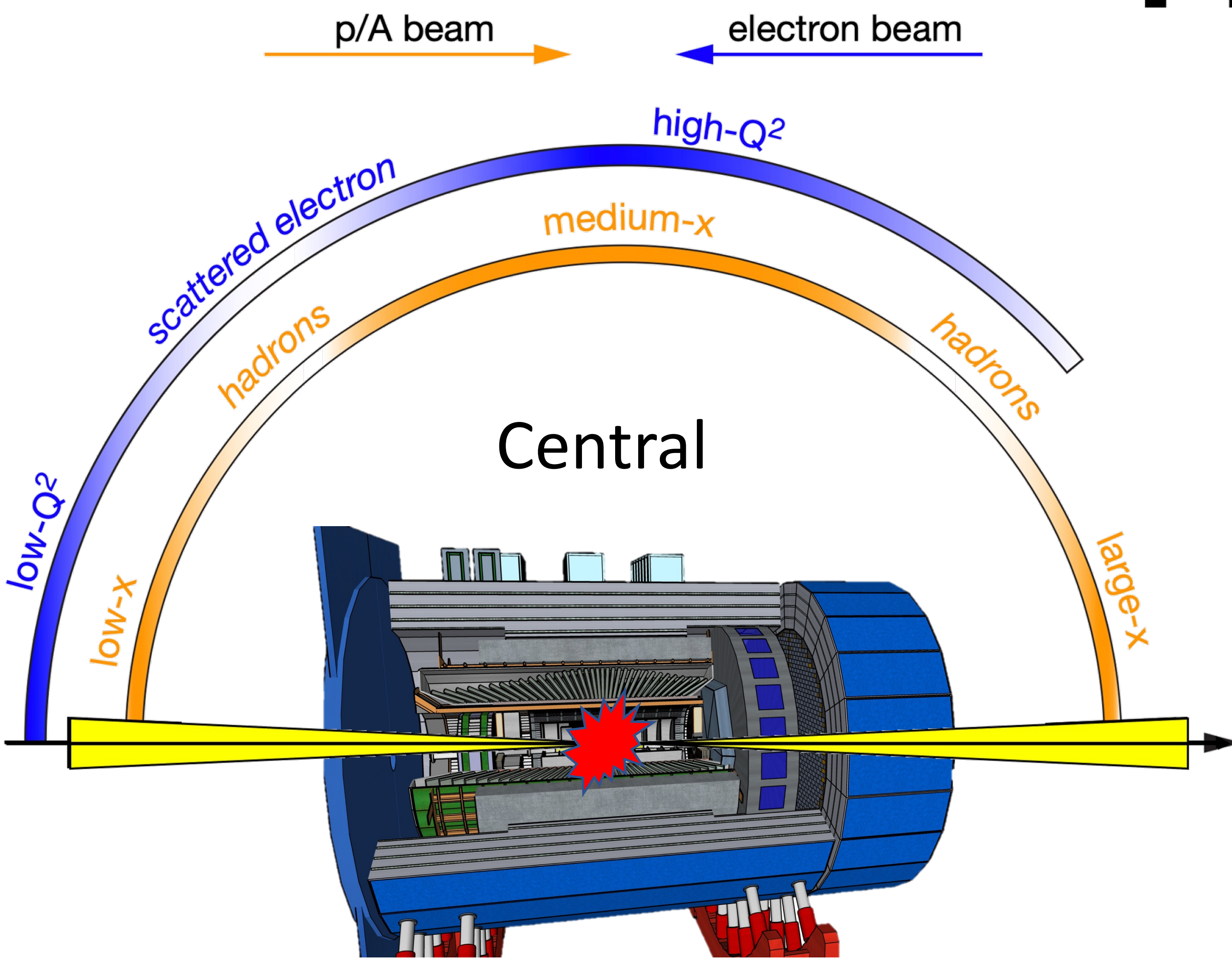

Angular distributions for DVCS

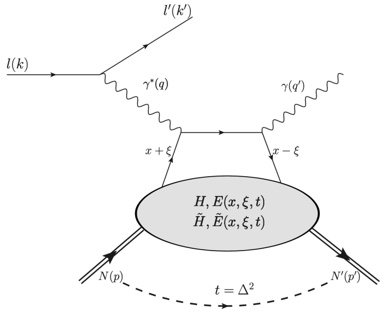

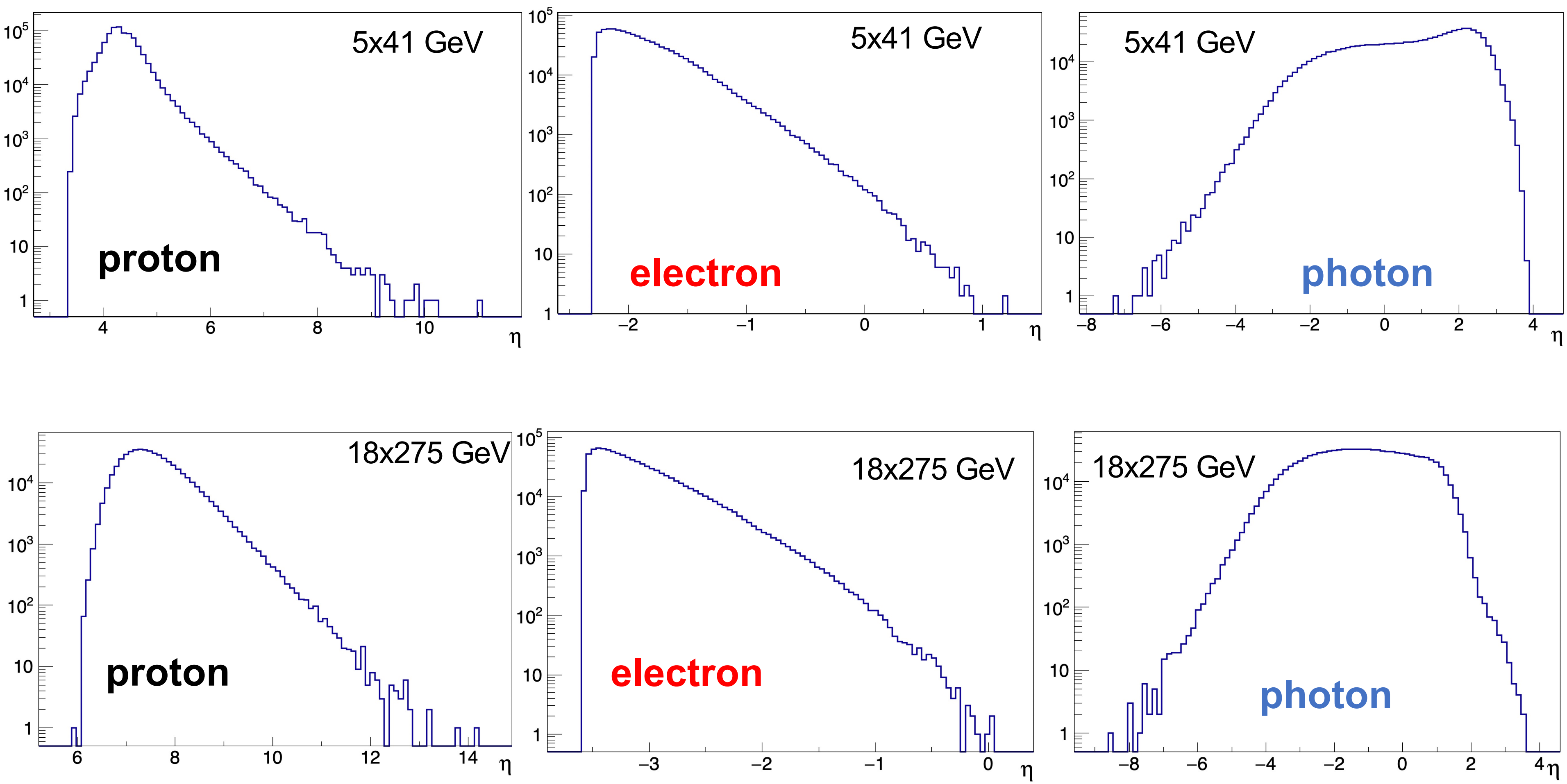

Angular distributions for DVCS

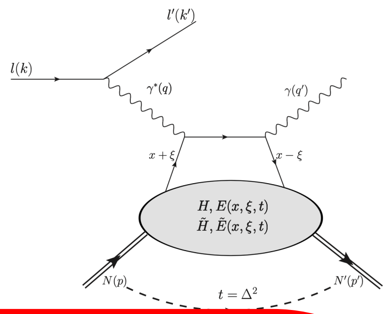

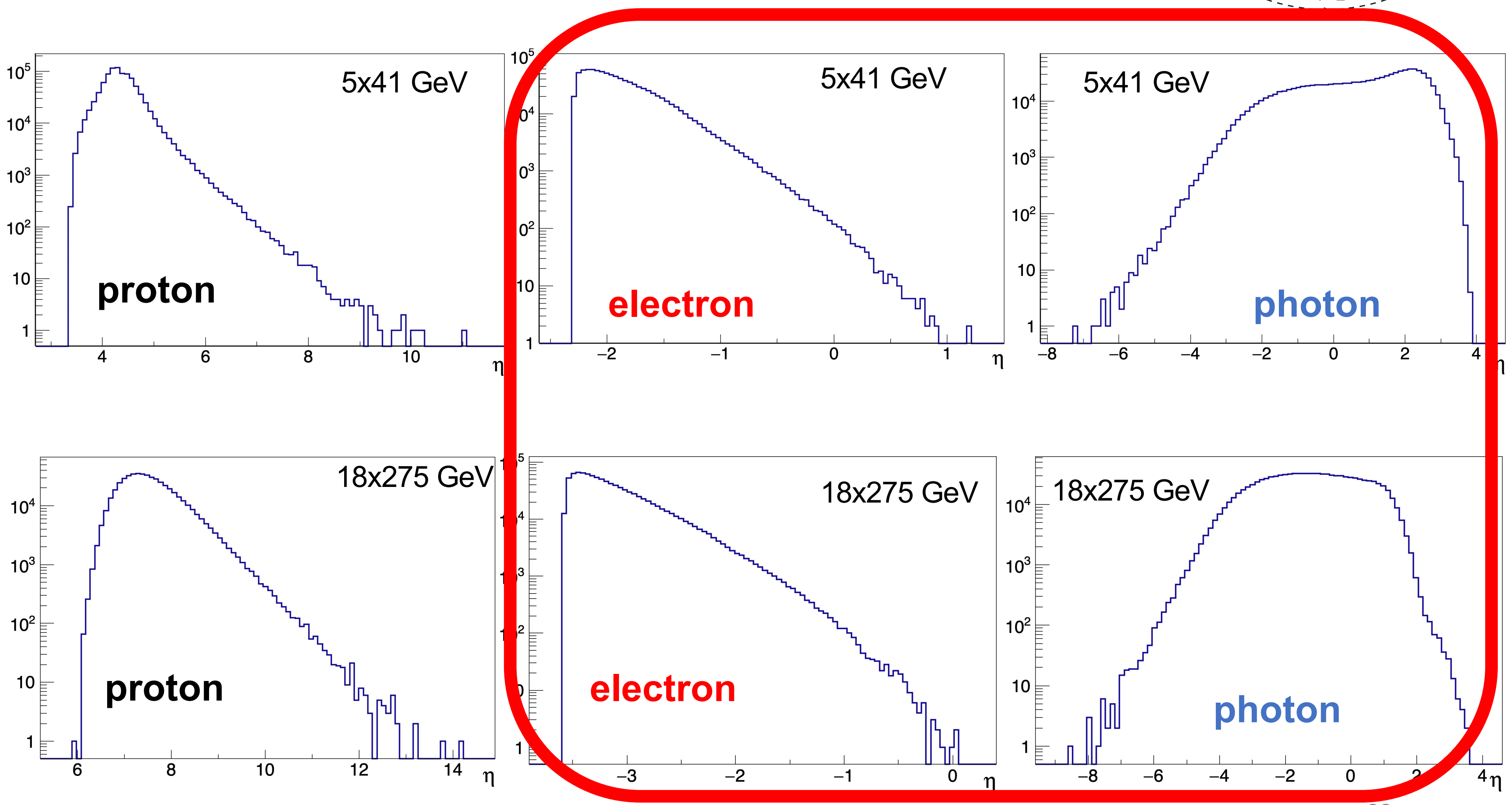

Detection Systems

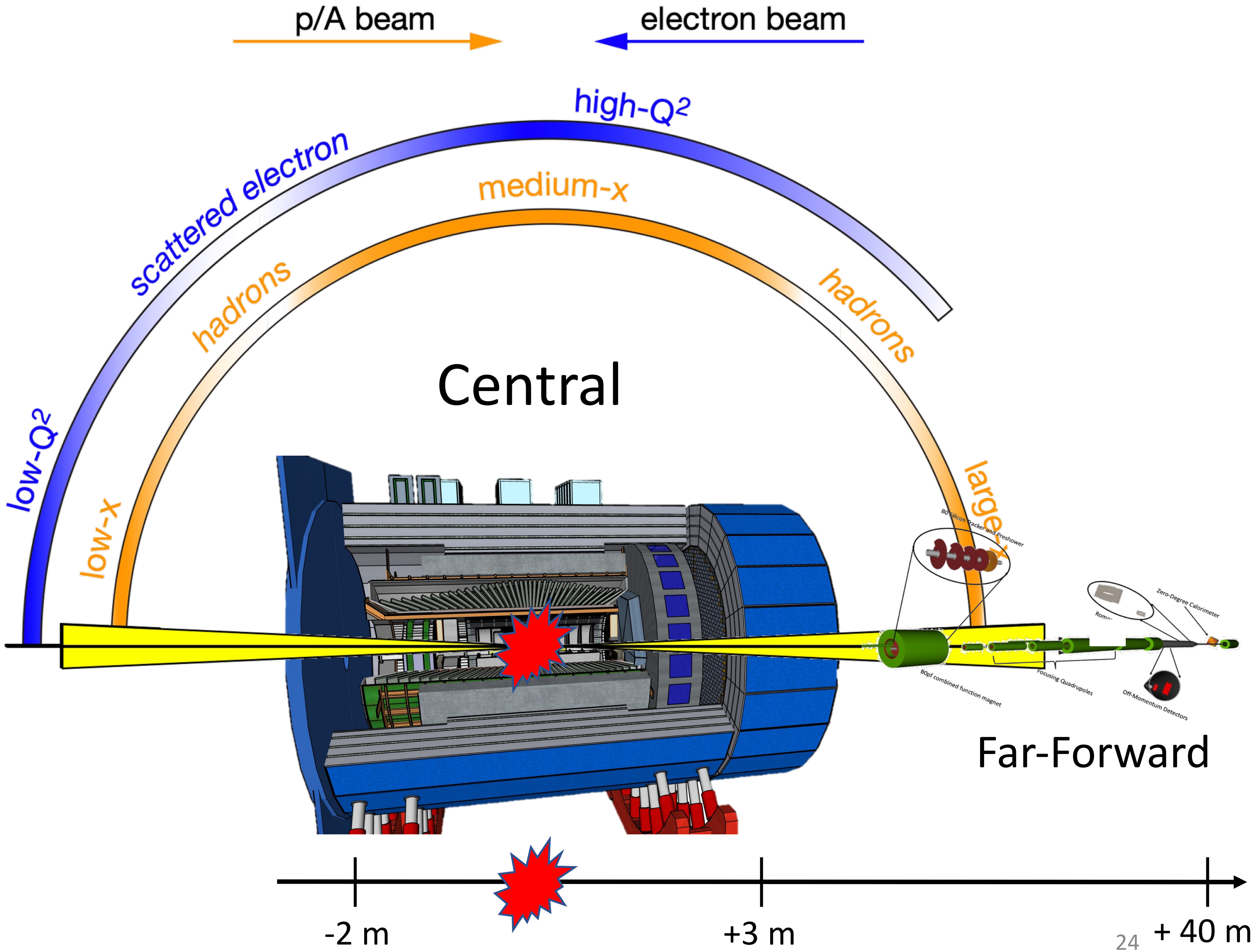

Far Forward Detectors

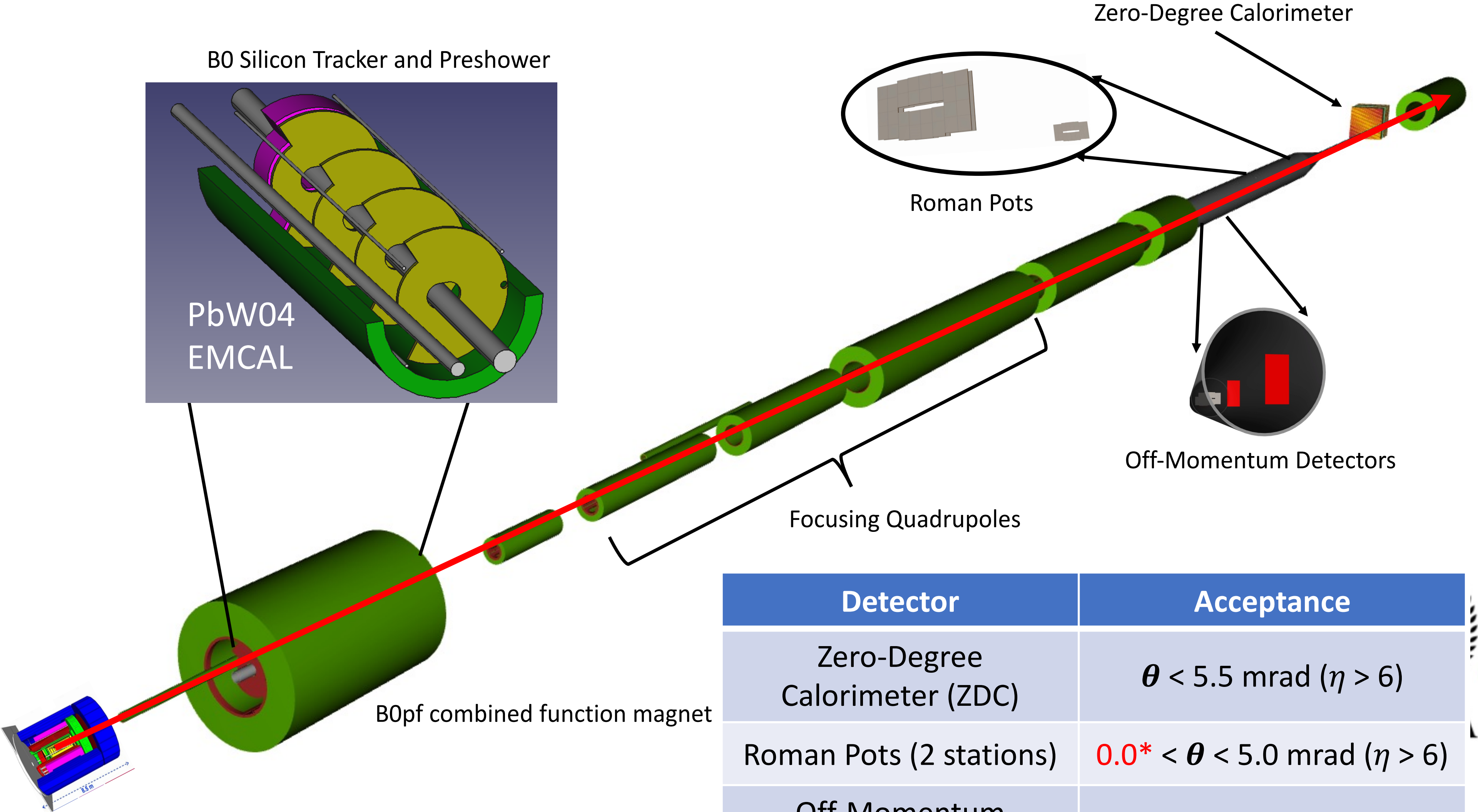

Detector	Acceptance
Zero-Degree Calorimeter (ZDC)	$\boldsymbol{\theta} < 5.5$ mrad ($\eta > 6$)
Roman Pots (2 stations)	0.0* < $\boldsymbol{\theta}$ < 5.0 mrad ($\eta > 6$)
Off-Momentum Detectors (2 stations)	$0.0 < \boldsymbol{\theta} < 5.0$ mrad ($\eta > 6$)
B0 Detector	$5.5 < \boldsymbol{\theta} < 20.0$ mrad ($4.6 < \eta < 5.9$)

Three Detection Systems

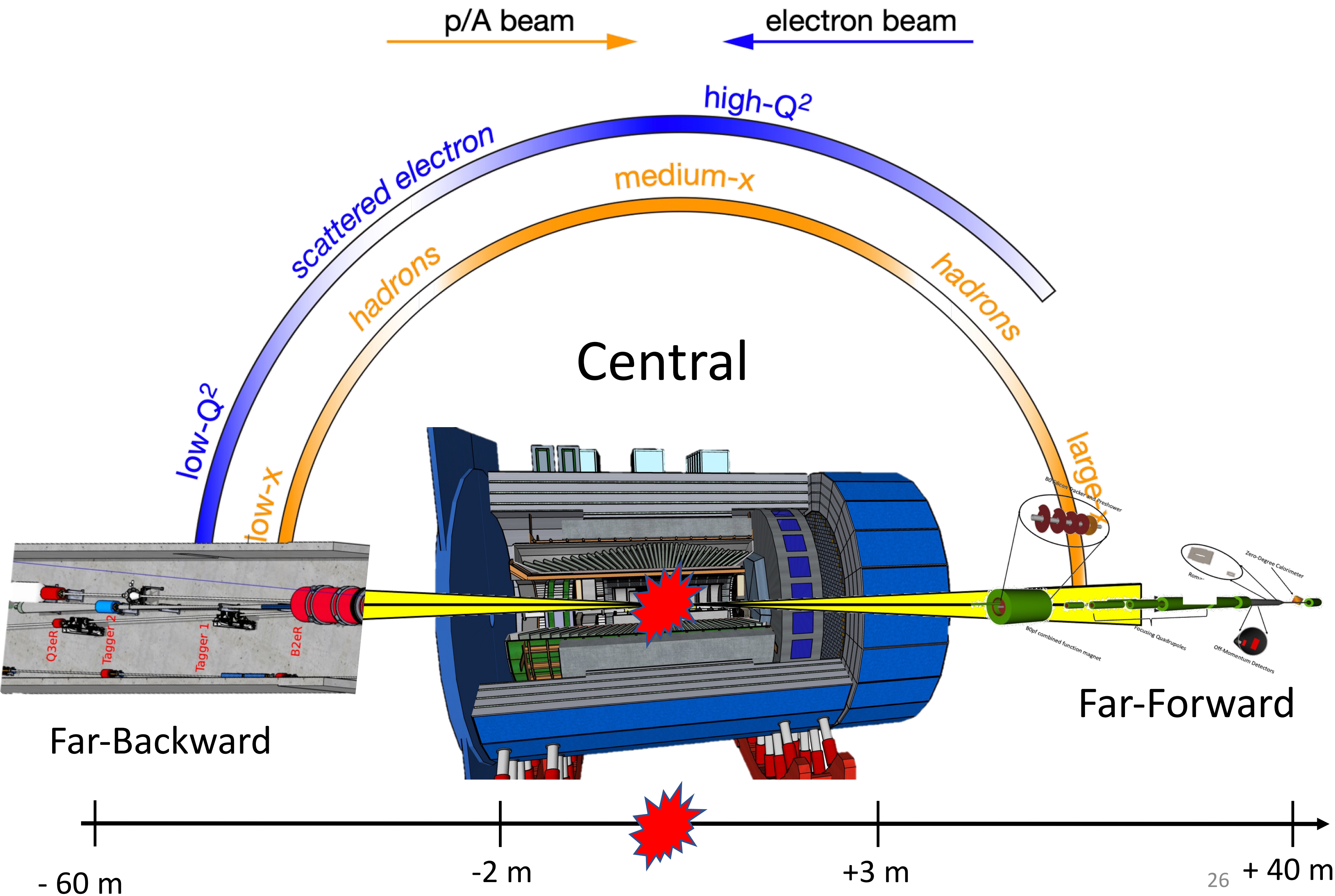

Far Backwards Detectors

Low-Q^2 tagger

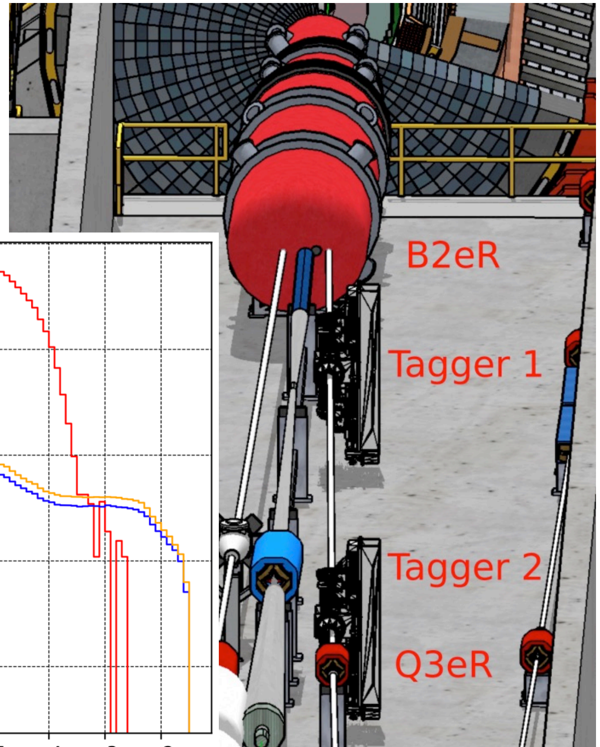

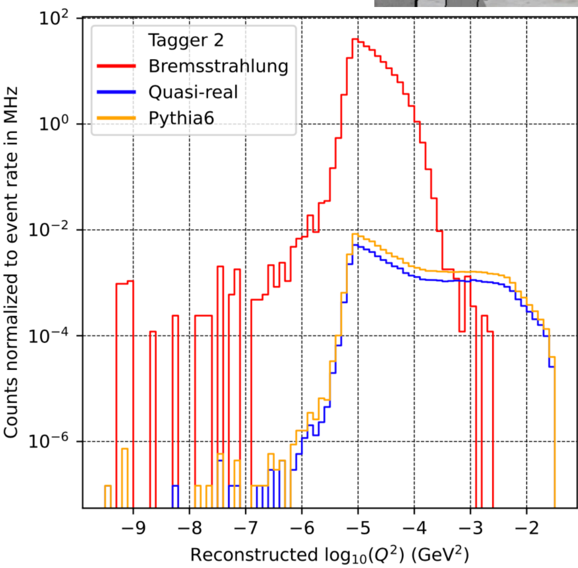

Clean photoproduction signal for $10^{-3} < Q^2 < 10^{-1}$

Luminosity Spectrometer

$e+p \rightarrow e\ \gamma\ p$

$e+Au \rightarrow e\ \gamma\ Au$

~1% measure of luminosity
relative luminosity to 10^{-4}

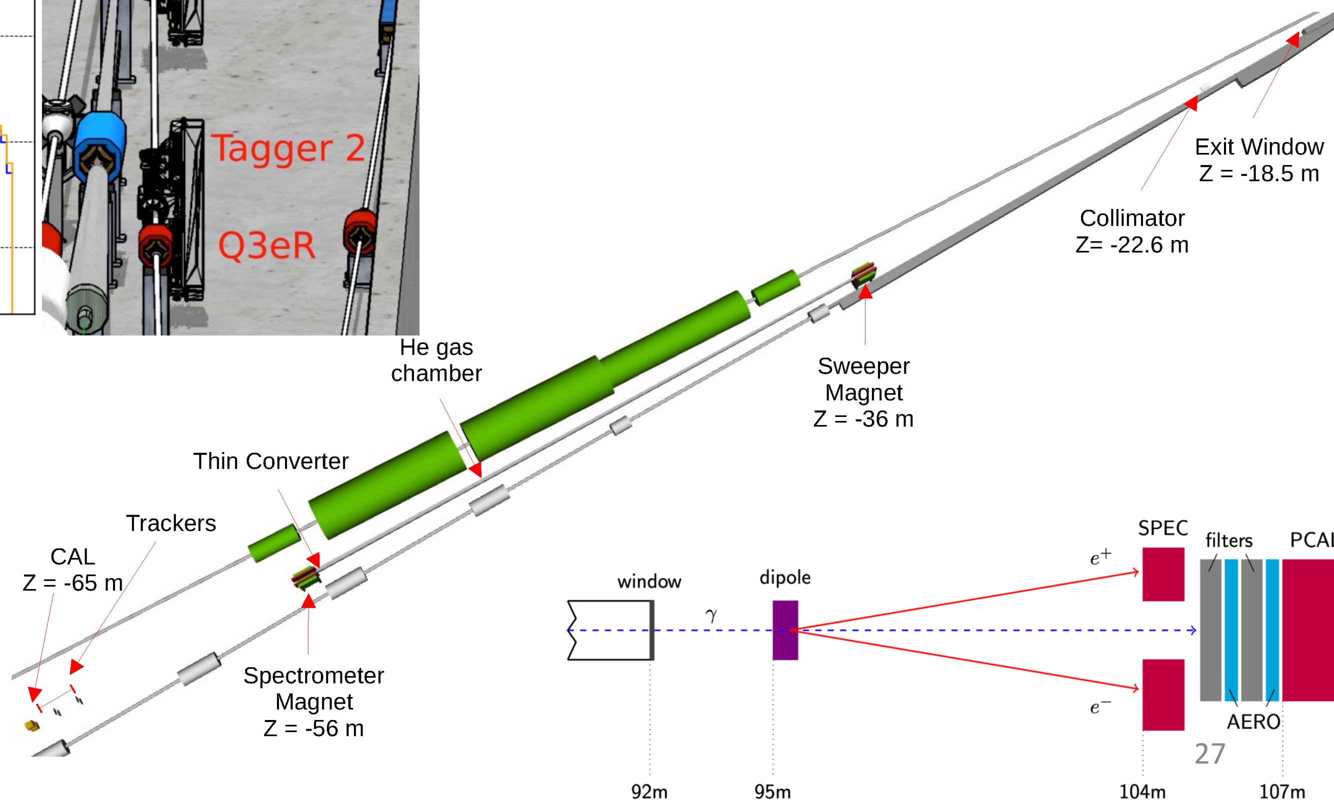

Simulation tool:

MILOU (3D) - generator https://arxiv.org/pdf/hep-ph/0411389v1.pdf

3D – lookup tables (Q^2,x_B,t) (interplay between all three variables)

KM – implemented in GeParD (Nucl.Phys.B794:244-323,2008)

GK – implemented in PARTONS (arXiv:1512.06174)

Improved generator (EpIC) *Eur. Phys. J. C* **82**, 819 (2022)

https://indico.cern.ch/event/1072533/contributions/4831030/attachments/2437404/4176605/DIS_2022.pdf Presentation by Kemal Tezgin

Weighted DVCS Phase Space @ ePIC

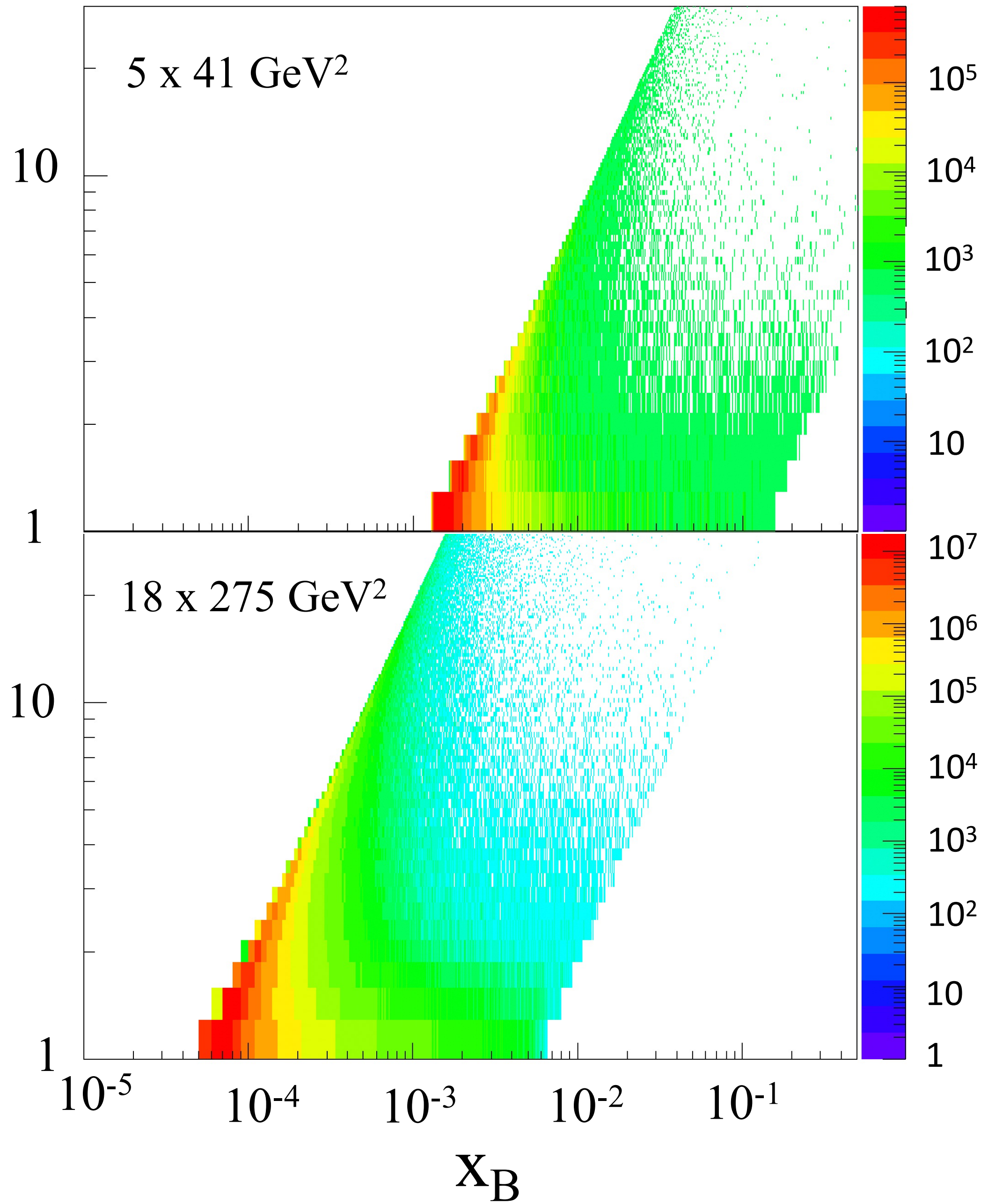

EpIC Generator based on:
[Eur. Phys. J. C 82, 819 (2022)]

Projected cross-sections

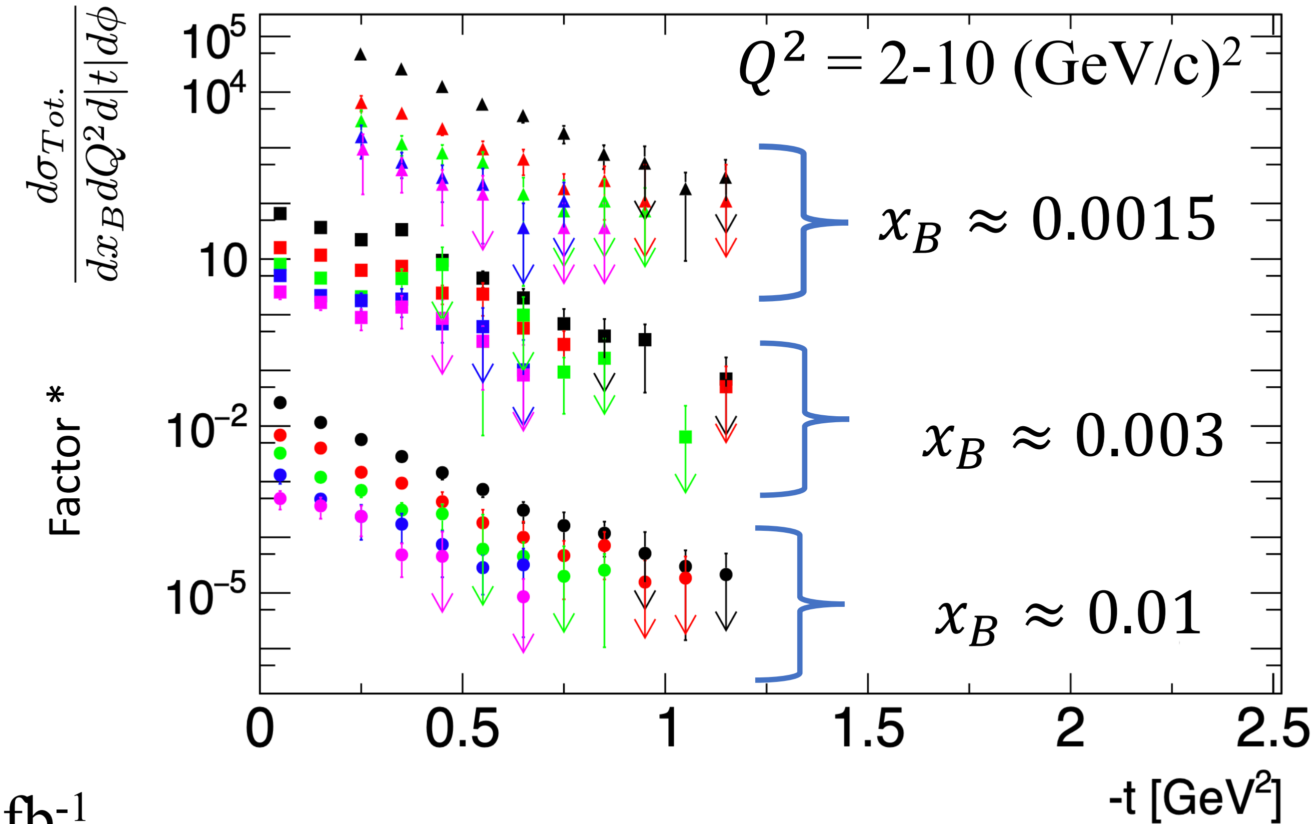

$\mathcal{L} = 10$ fb^{-1}

ECCE Simulation

▲ e+p 18+275 GeV

■ e+p 10+100 GeV

● e+p 5+41 GeV

5x41 GeV^2

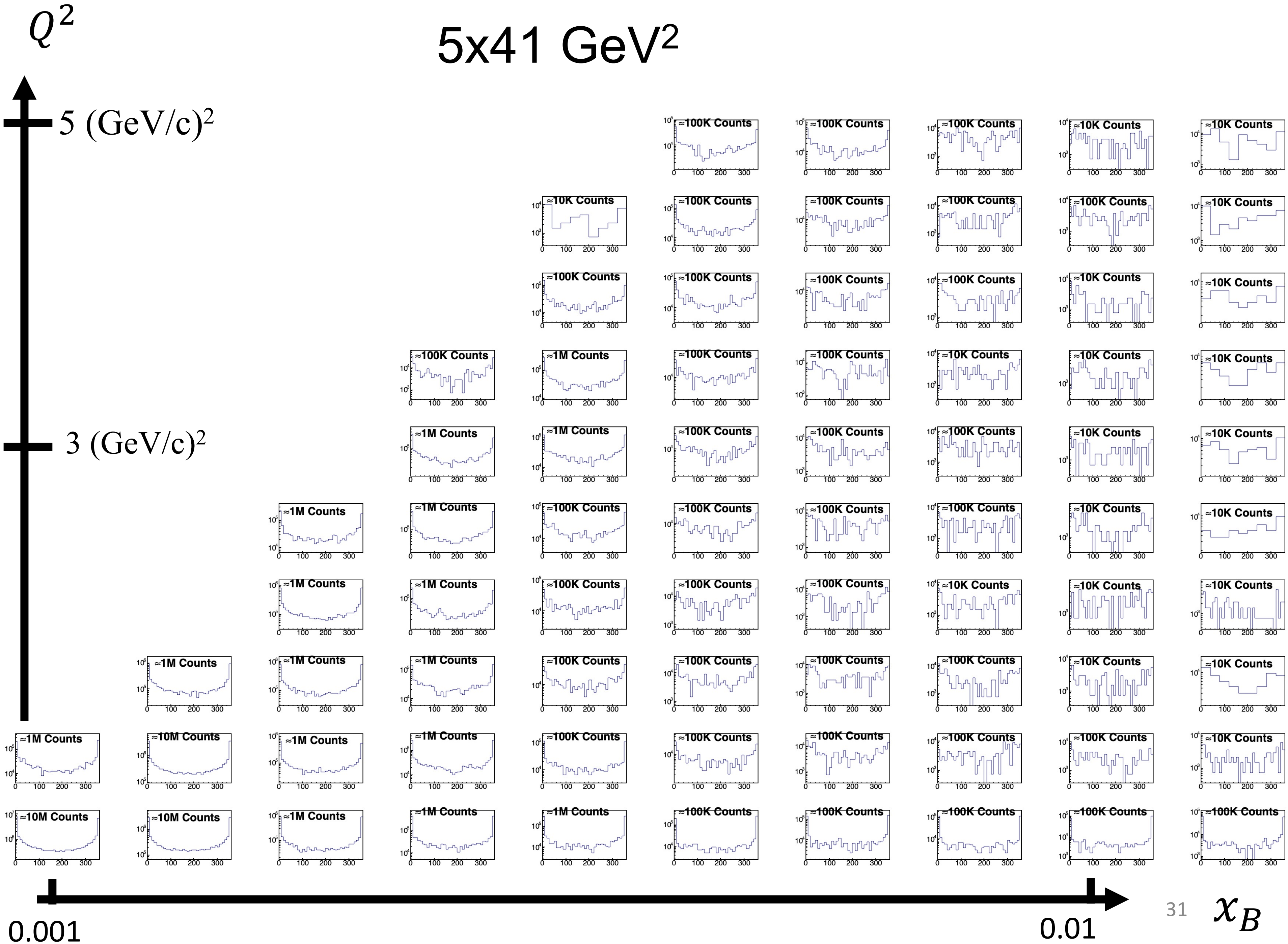

Q²
5 (GeV/c)²
3 (GeV/c)²
≈10K Counts ≈100K Counts ≈100K Counts ≈100K Counts ≈100K Counts
≈10K Counts ≈100K Counts ≈100K Counts ≈100K Counts ≈100K Counts ≈10K Counts
≈100K Counts ≈100K Counts ≈100K Counts ≈100K Counts ≈10K Counts ≈10K Counts
≈100K Counts ≈1M Counts ≈100K Counts ≈100K Counts ≈10K Counts ≈10K Counts ≈10K Counts
≈1M Counts ≈1M Counts ≈100K Counts ≈100K Counts ≈100K Counts ≈10K Counts ≈10K Counts
≈1M Counts ≈1M Counts ≈100K Counts ≈100K Counts ≈100K Counts ≈100K Counts ≈10K Counts ≈10K Counts
≈1M Counts ≈1M Counts ≈100K Counts ≈100K Counts ≈100K Counts ≈10K Counts ≈10K Counts ≈10K Counts
≈1M Counts ≈1M Counts ≈1M Counts ≈100K Counts ≈100K Counts ≈100K Counts ≈100K Counts ≈10K Counts ≈10K Counts
≈1M Counts ≈10M Counts ≈1M Counts ≈1M Counts ≈100K Counts ≈100K Counts ≈100K Counts ≈100K Counts ≈100K Counts ≈10K Counts
≈10M Counts ≈10M Counts ≈1M Counts ≈1M Counts ≈1M Counts ≈100K Counts ≈100K Counts ≈100K Counts ≈100K Counts ≈100K Counts
0.001
0.01
x_B

Q^2

18 x 275 GeV^2

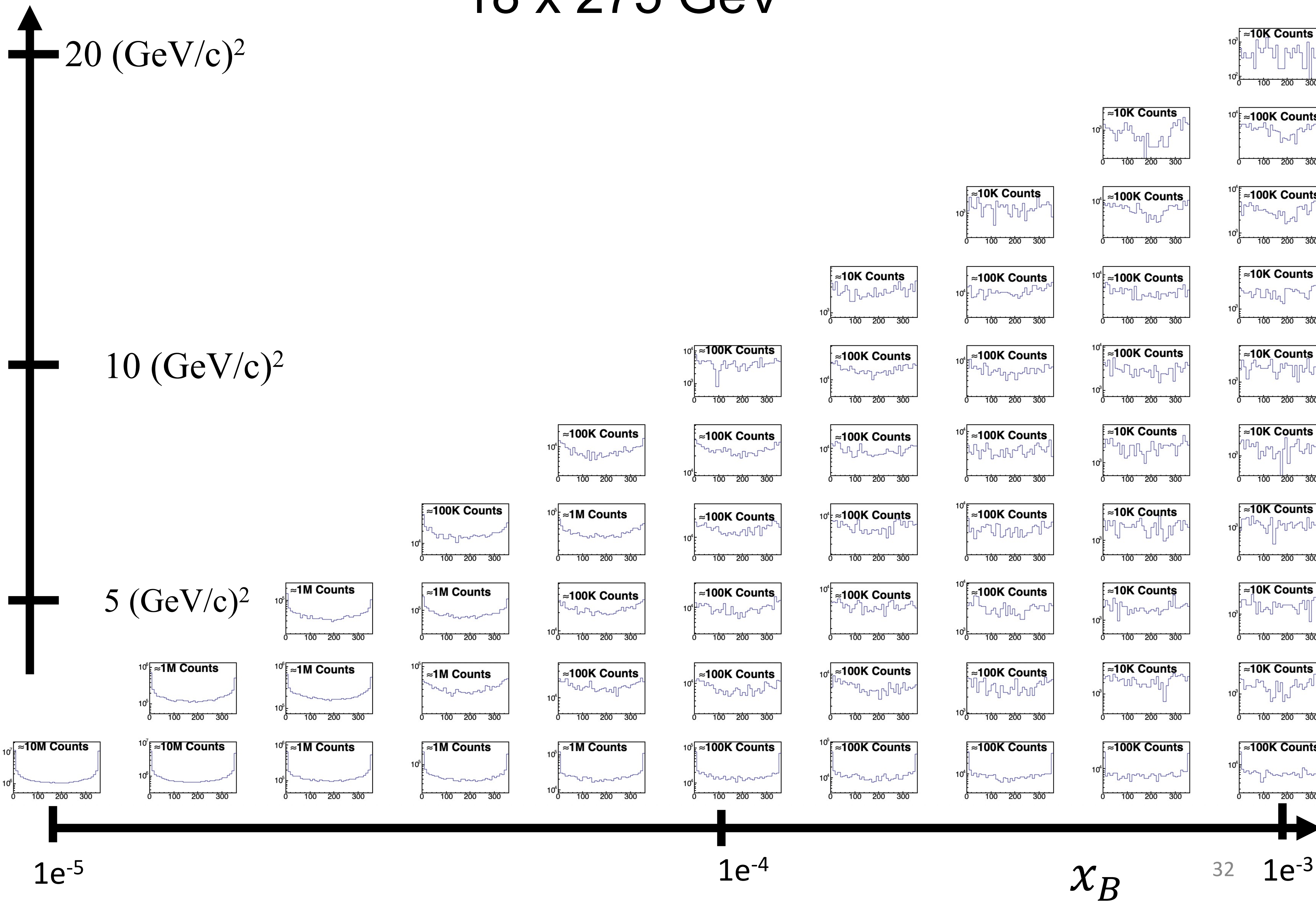

18 x 275 GeV^2

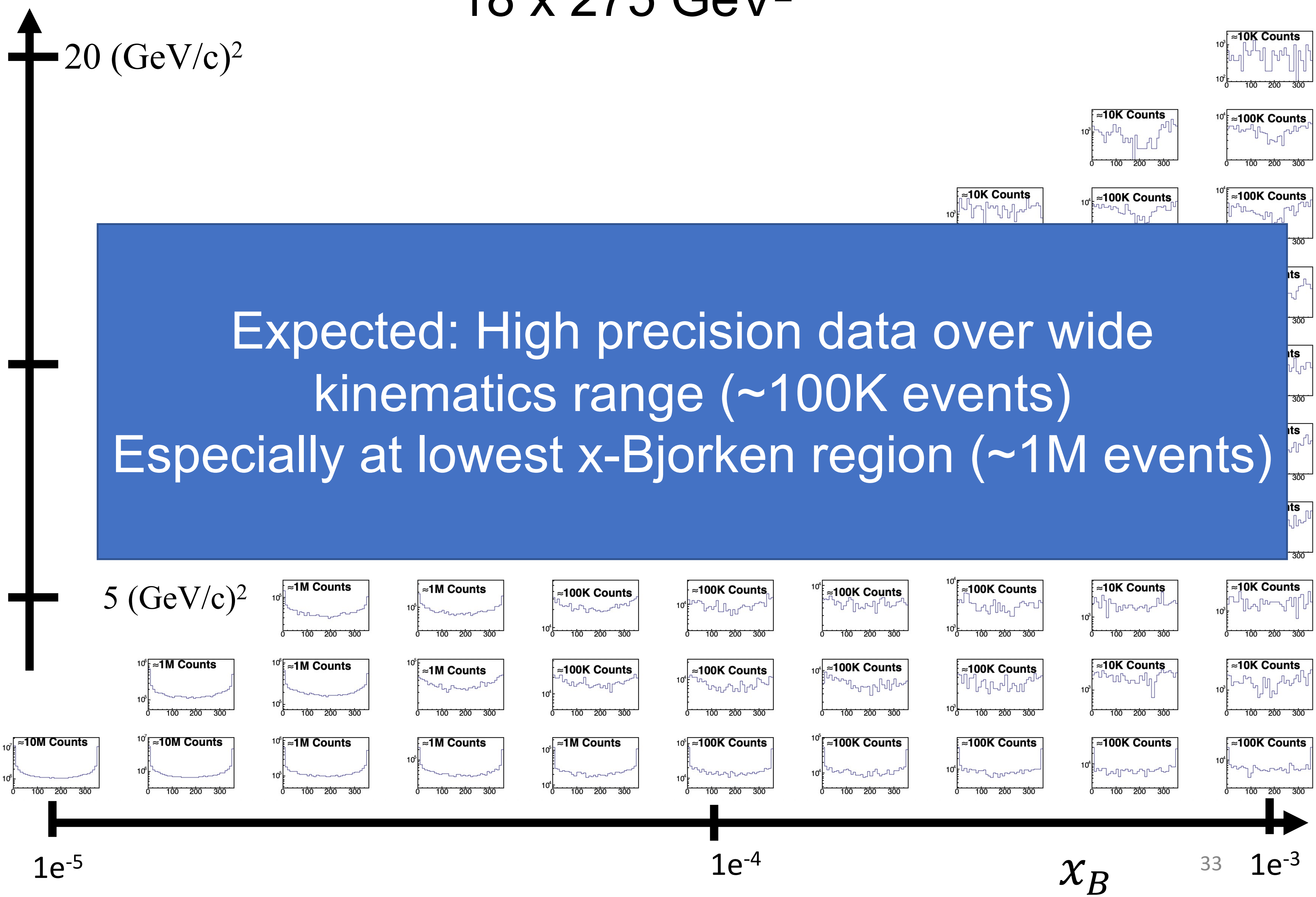

Expected: High precision data over wide kinematics range (~100K events)
Especially at lowest x-Bjorken region (~1M events)

π^0 Background

$$e + p \rightarrow e' + p' + \pi^0(\gamma\,\gamma)$$

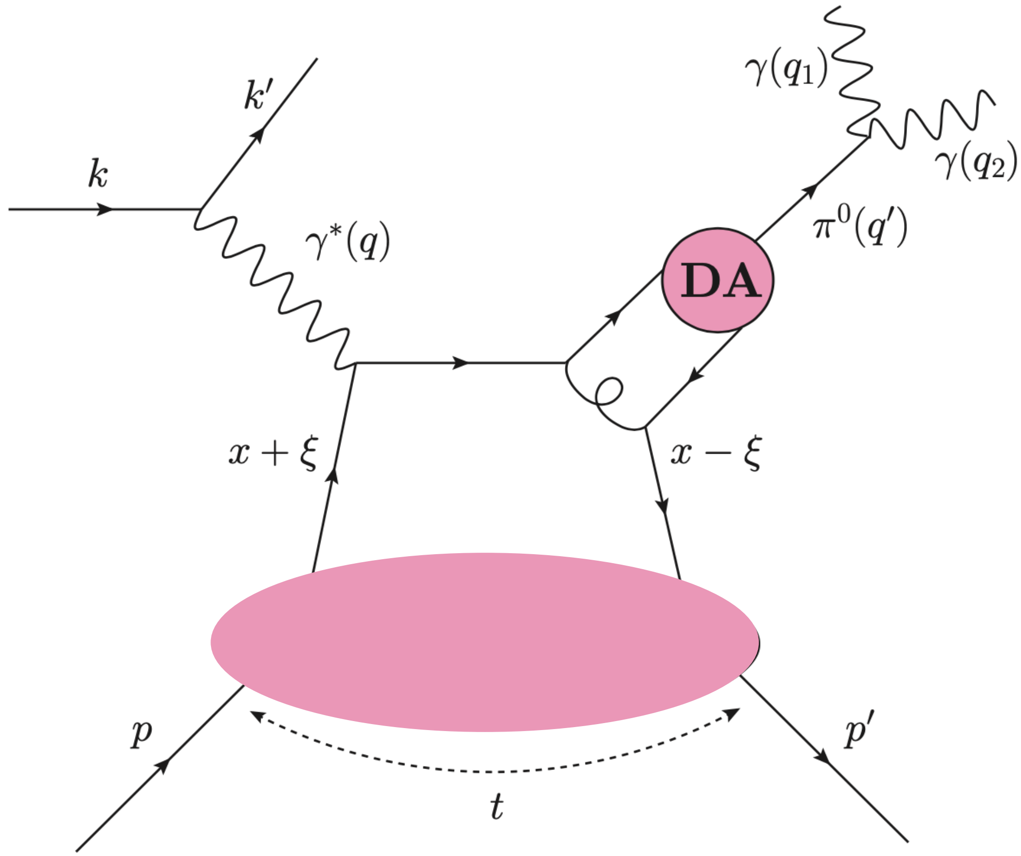

π^0 contamination at EIC kinematics: Significant at low-energy and high pseudo-rapidity

5x41 GeV^2 | 18x275 GeV^2

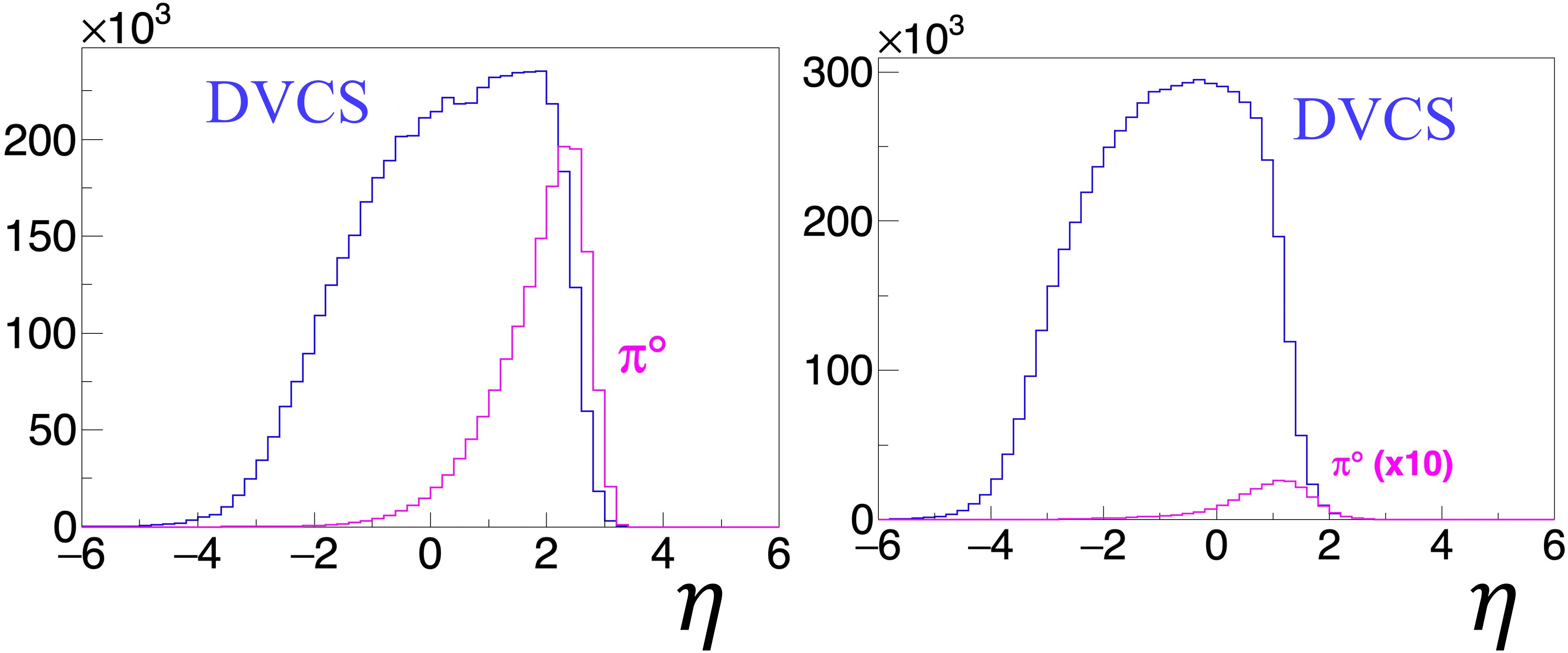

Normalized to $\mathcal{L} = 10\ fb^{-1}$

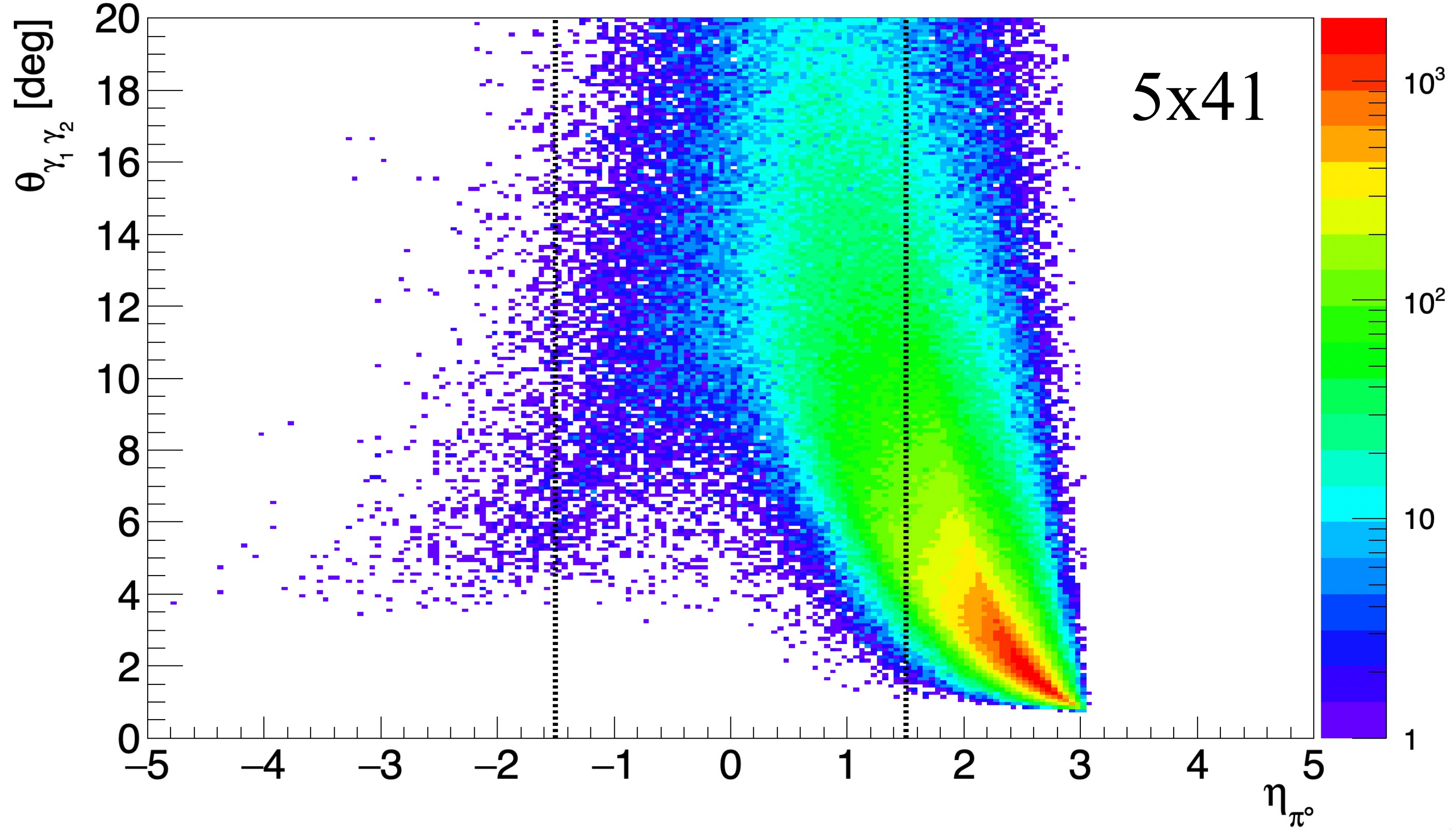

5x41
$\theta_{\gamma_1\gamma_2}$ [deg]
η_{π°

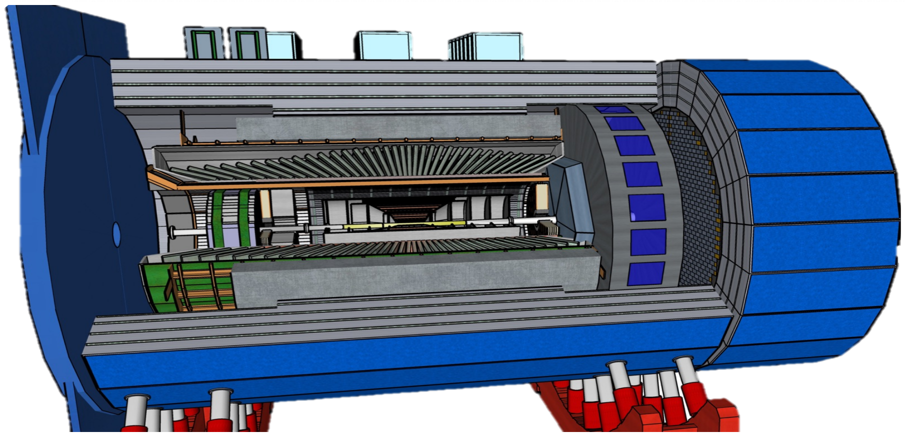

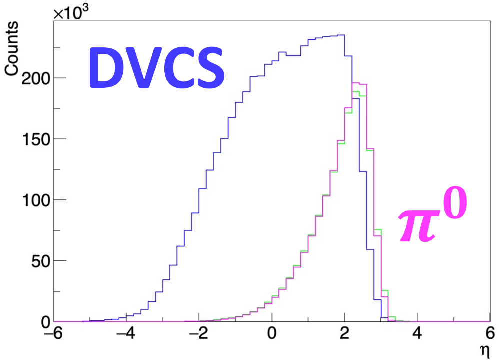

DVCS
π^0
Counts
η

Photon detection

Generate photons

Detector Simulation

Clustering

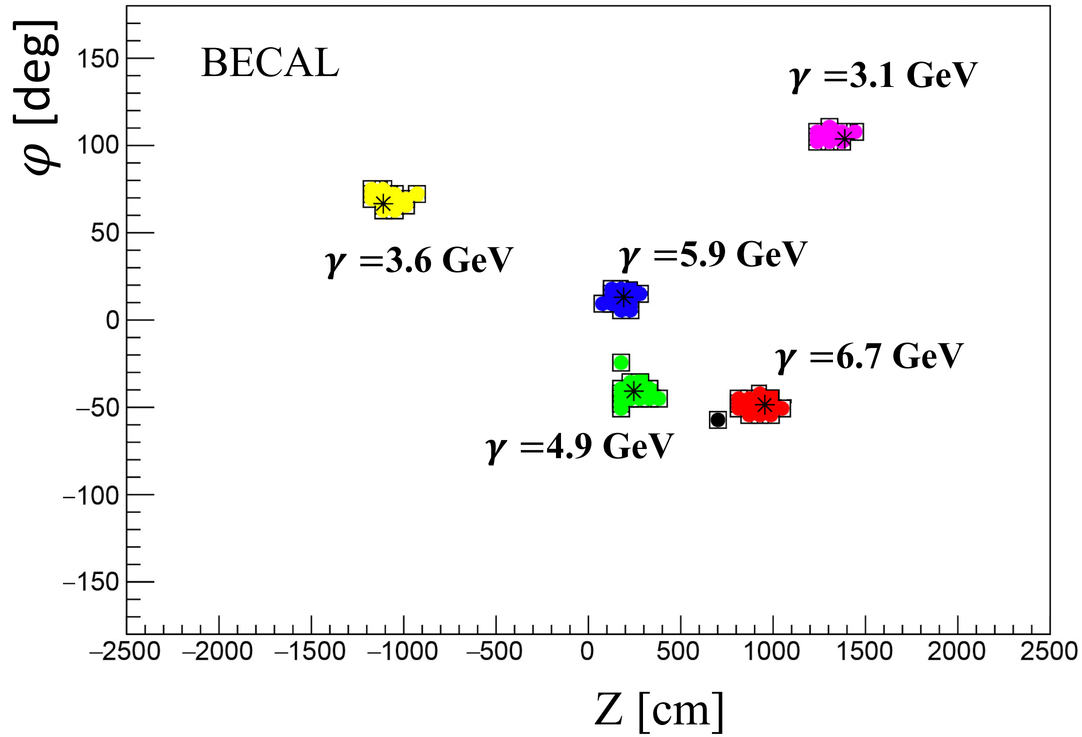

➔
1) Energy Resolution
2) Angular Resolution
3) Acceptance

Endcap Angular Resolution: ~ 0.1 [deg]

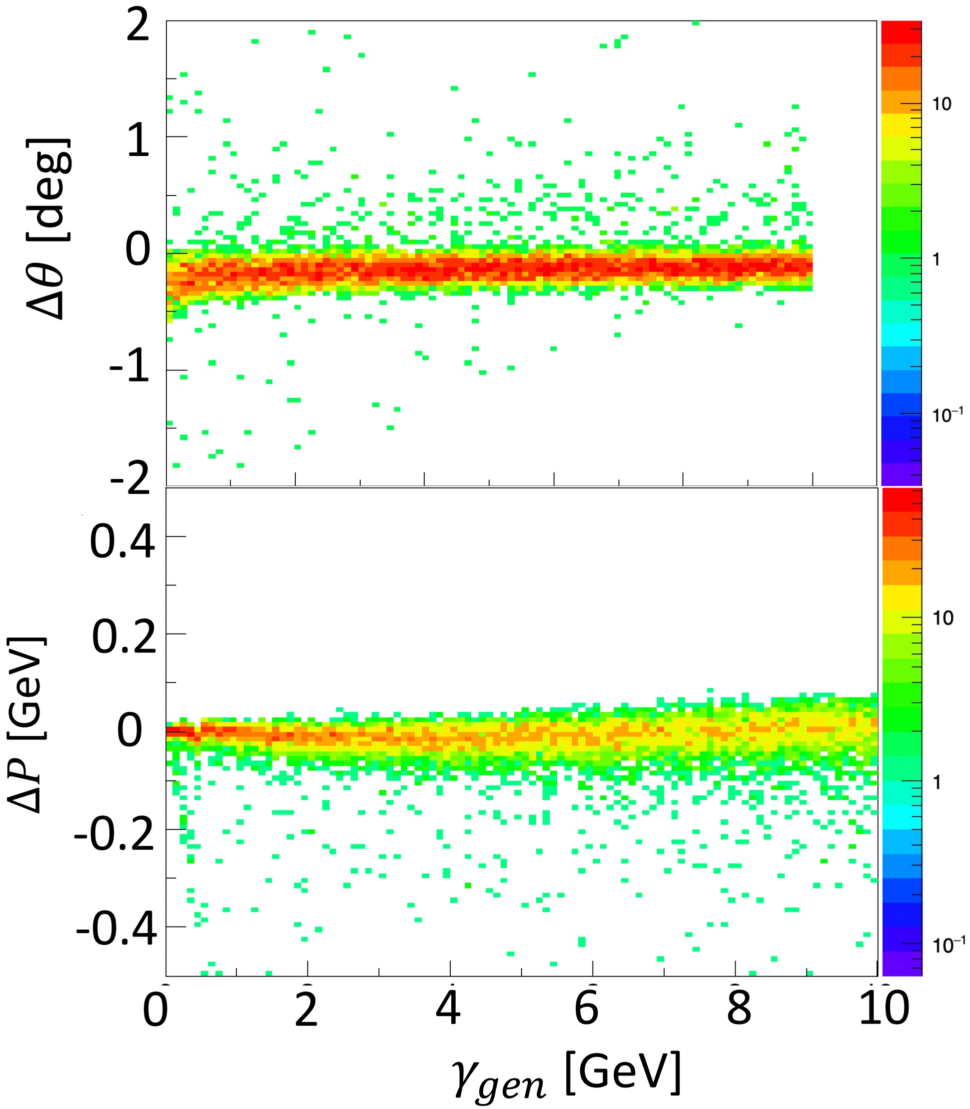

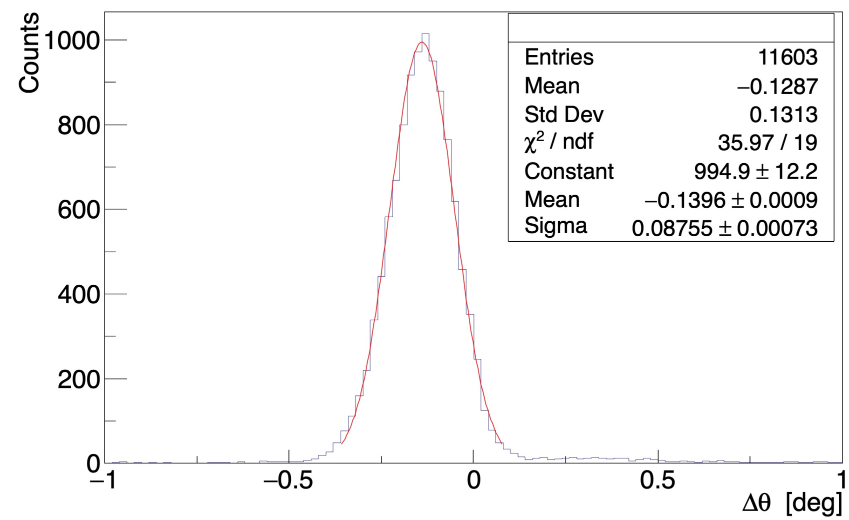

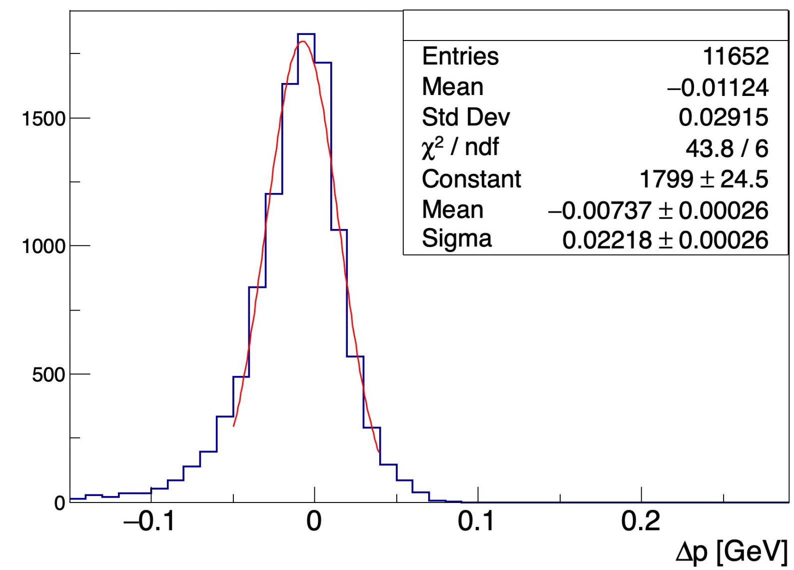

(not including vertex uncertainties etc.)

Pion reconstruction including detector resolution

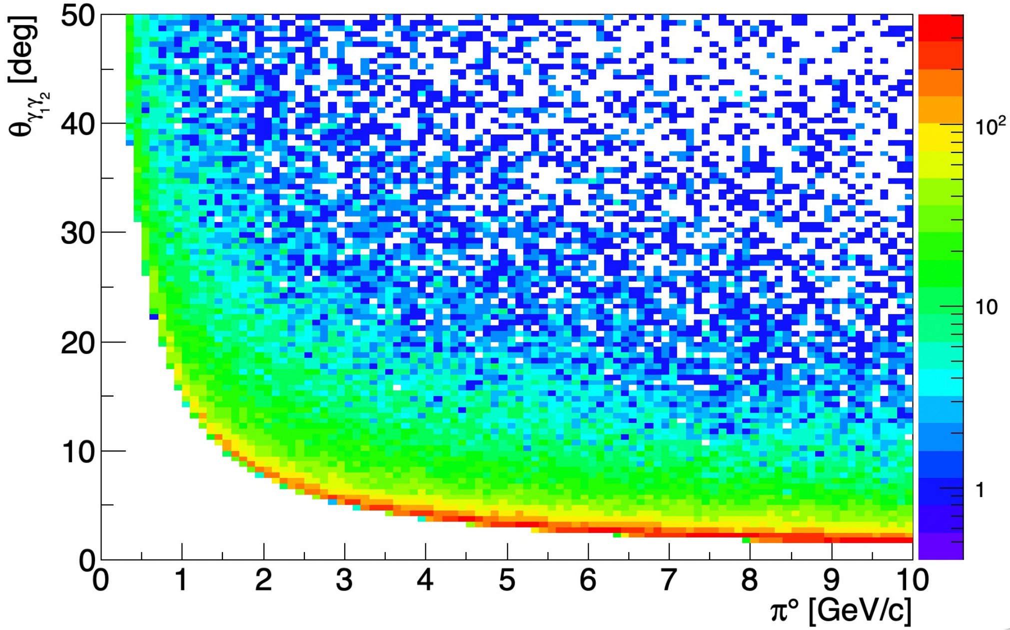

Simulated pions

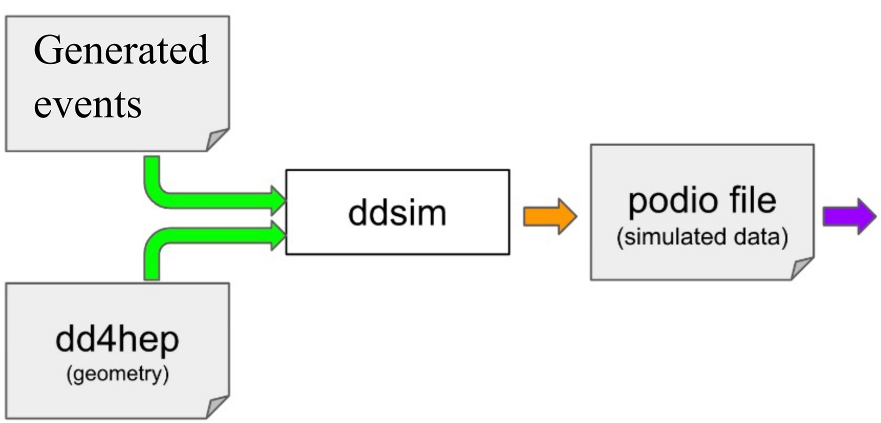

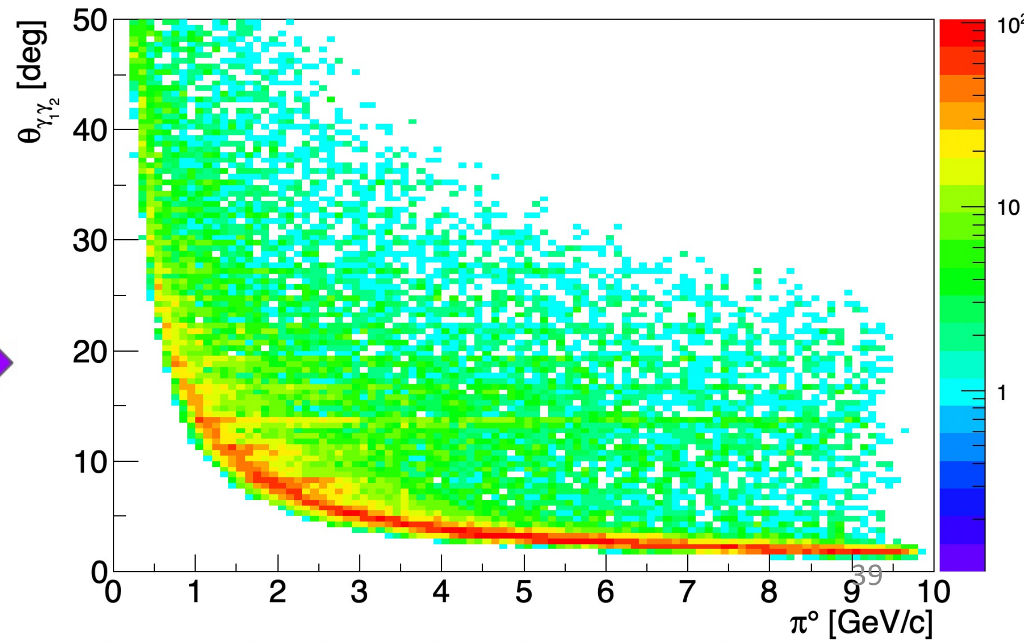

5x41

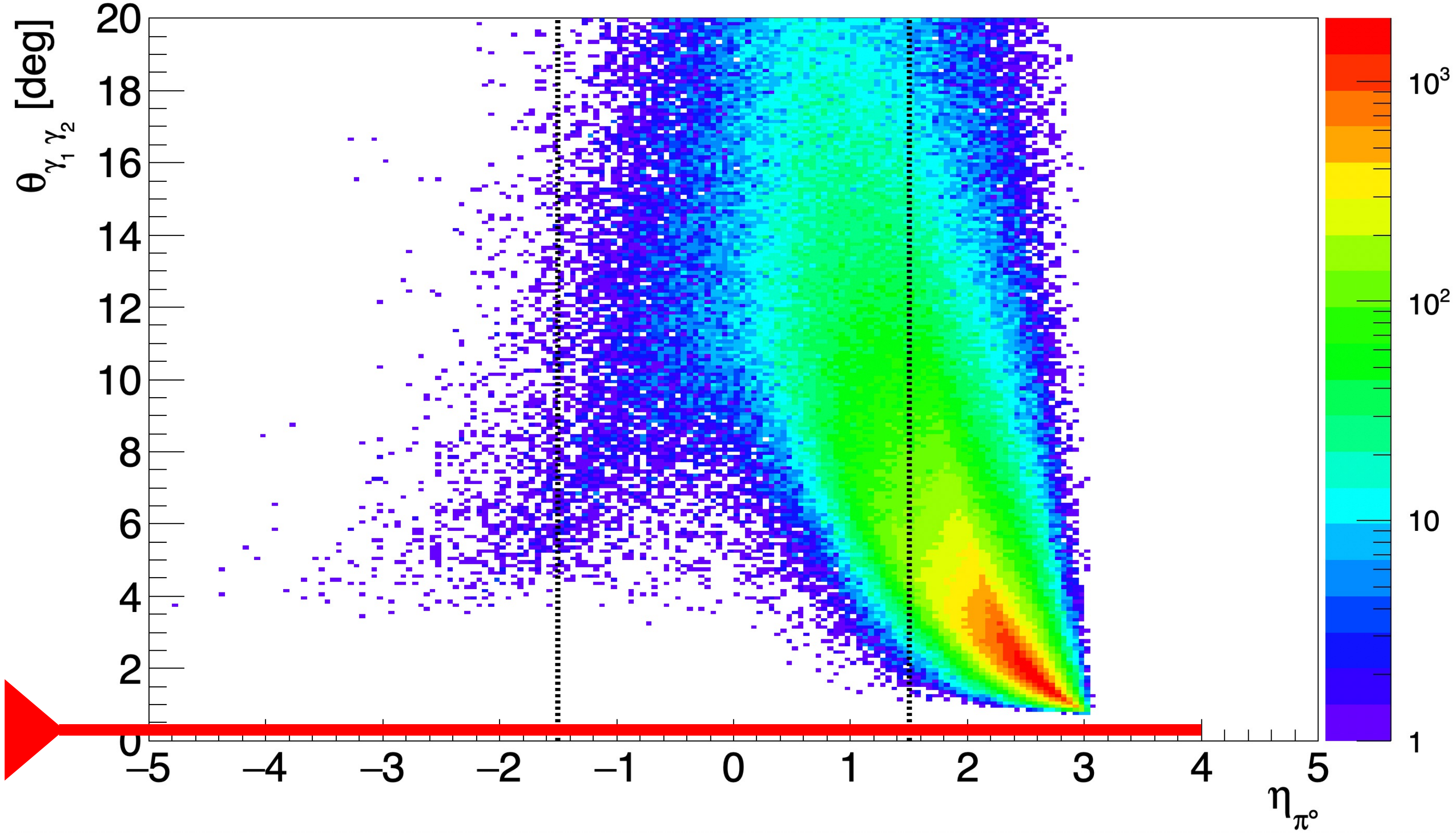

$\theta_{\gamma_1 \gamma_2}$ [deg]
20
18
16
14
12
10
8
6
4
2
0
−5
−4
−3
−2
−1
0
1
2
3
4
5
η_{π°
10^3
10^2
10
1

Summary

- EIC will provide a wide phase space for DVCS study.

→ Probe low x-Bjorken sector

- High precision data is expected over the wide kinematical range.

→ Crucial for multidimensional analysis

- Significant improvement in GPD H and sensitivity to GPD E

- Mapping transverse parton distribution

Thank you!